Damage in metal forming

A.E. Tekkaya, Pierre-Olivier Bouchard, S. Bruschi, C.C. Tasan

Damage in metal forming

A.E. Tekkaya[a,*], P.-O. Bouchard[b], S. Bruschi[c], C.C. Tasan[d]

[a]Institute of Forming Technology and Lightweight Components (IUL), TU Dortmund University, Dortmund, Germany
[b]MINES ParisTech, PSL Research University, CEMEF Centre de mise en forme des matériaux, Sophia Antipolis, France
[c]Department of Industrial Engineering, University of Padova, Padova, Italy
[d]Department of Materials Science and Engineering, Massachusetts Institute of Technology, Cambridge, USA

Physical mechanisms of ductile damage in metal forming, experimental characterization methods for dam-age, and models predicting the damage level in formed components are reviewed. Applications of damage analysis in metal forming processes reveal that damage in metal formed parts is not failure, but a product property that accumulates between processes. Various metal forming process designs demonstrate that dam-age in formed products can be reduced and their performance can be increased. Static and fatigue strength, impact toughness, stiffness, and formability are typical examples of performance indicators that can be improved by damage-based process design. Potential scientific and technological challenges are addressed to realize damage-controlled metal forming processes.

1. Introduction

Metal forming influences product properties [199]. These product properties determine the performance of the component during service loading or during further manufacturing steps. The better the knowledge about the properties of the product after forming, the lower the safety factor for the use of the component in service can be set. The safety factor is defined as the material's capability divided by the applied load. The material's capability is influenced by the manufacturing process. Knowing the work-hardening, for instance, of any formed component allows a better prediction of its strength, lowering of the safety factor, and, finally, reducing the mass of the component. Therefore, it is a primary goal to predict and influence the product properties by manufacturing for reducing the safety factors and, hence, reducing the weight of the component. The conventional properties impacted by forming are the work-hardening (strength and hardness) and the residual stresses of the product. Both of these mechanical properties influence the static strength [110], the fatigue strength [214], the impact strength [220], the corrosion behavior [204] etc. of the product. However, there is an additional important property of the product that is not recognized in the assessment of formed components: the damage level of the component.

Damage has been associated in history with fracture and hence failure. Failure of iron wires has been tested firstly by Leonardo de Vinci in the 15th century as documented in his note "Testing the strength of Iron Wires of Various Length". He found that shorter wires support more weight under tension than longer wires with the same diameter. This conflicts with the expectations of the macroscopic strength of materials based on the continuum assumption. Yet, noticing that the number of microscopic defects in wire could increase with its length, this very early observations deliver a first indication of the importance of the microstructure in considering failure [129]. The strength of beams under bending has been analysed by Galileo Galilei in the 17th century leading to the importance of internal bending moments. These studies have been followed by various strength hypotheses in the 19th century some of which even survive today as failure criteria.

Ludwik [127] documented in 1926 a round unbroken aluminium tension specimen exhibiting a crack in the centre of the neck (Fig. 1a). This was the first indication that a component plastically formed, and apparently not failed, may have some sort of discontinuity, here a crack, inside it. In an even earlier paper Ludwik and Scheu [128] indicated the effect of stress state on the amount of plastic strain until failure by analysing tension specimens with various notches. In 1930, Remmers [162] detected in drawn wires made of copper and aluminium Chevron cracks with differently sized pores between them at the centre of the wire (Fig. 1b). He found that

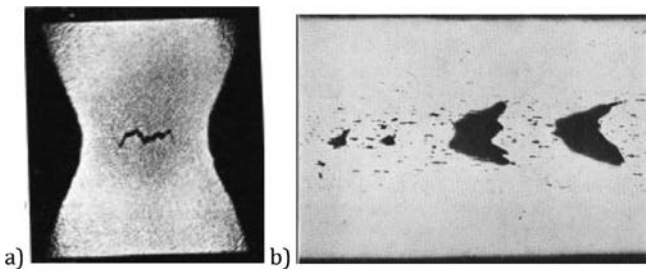

Fig. 1. a) An internal crack in a tensile specimen made of pure aluminium necked by 80% area reduction, [127]. b) Chevron cracks and holes between the cracks at the centre of a copper wire drawn in 8 successive dies with a total area reduction of 67.6%, [162]. Void coalescences between the Chevron cracks of various sizes are seen clearly.

* Corresponding author.
E-mail address: erman.tekkaya@iul.tu-dortmund.de (A.E. Tekkaya).

fracture was promoted by low drawing die angles and low area reductions as well as higher oxygen content in the workpiece material. Investigating the fracture of mild steel specimens under tensile loading, Tipper [200] observed that micro-holes nucleated in the unfractured parts of the specimen, which have later been named voids.

Bridgman [26] showed in his ground-breaking study that during simple tension tests of various metals such as steel, aluminium, copper, brass, and bronze both the strain at fracture as well as the nature of the fracture changed with superimposed hydrostatic pressure (Fig. 2).

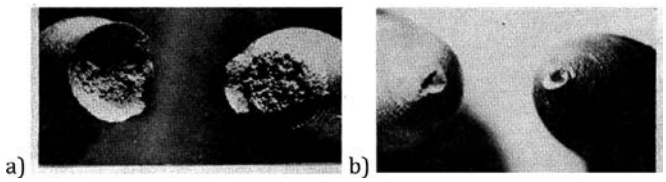

Fig. 2. Fracture surfaces of the same steel specimen broken (a) at atmospheric pressure and (b) at 1850 MPa hydrostatic pressure [26].

These fundamental findings have been the basis for the discovery of the mechanisms of ductile damage based on void nucleation/growth/coalescence with and without instability. This entire process and typical examples of each phenomena are illustrated in Fig. 3.

Despite all formed parts have a certain level of damage, they are still functionally acceptable parts. However, the damage level induced in a formed component can affect its service performance under various types of loads. Generally, the higher the tensile hydrostatic stress, the larger are the voids in size and, hence, the more damage is induced by plastic deformation in the material [136,163]. The loading paths and therefore the damage evolution, could be influenced by the metal forming process design and the resulting product performance as shown in [198]. This is a paradigm change in metal forming process design since conventionally, although the negative influence of damage is known, its consequences have been usually ignored during the process development.

Besides reviewing the state of the art, this paper aims at revealing a new process design approach in metal forming for minimum damage in the components. First, the physical mechanisms of damage initiation and evolution are discussed in Section 2. This is followed by the experimental characterization of damage in Section 3. The modeling of damage is detailed in Section 4. Section 5 is devoted to the application of damage models for failed components. Here, the evolution of damage until its limit is considered. In contrast, Section 6 describes the applications to determine the damage of not failed parts after metal forming and the effect of the damage level on the product properties in service or in a subsequent manufacturing process. In Section 7 industrial utilization of the described damage knowledge is compiled. Finally, new research fields and possible developments regarding damage-controlled metal forming processes are discussed in Section 8.

2. Mechanisms of ductile damage

Defining damage is not straightforward. In a broad sense it represents undesired evolution of one or more structural characteristic(s) that hinder(s) an engineering capability. In case of metal forming, the unwanted evolution is generally considered to be that of plastic straining-induced discontinuities in the volume of the material, e.g. micro-cracks or micro-voids. These ductile damage incidents nucleate at particular microstructural features, propagate further and coalesce, ultimately leading to fracture. This particular definition of damage is based on the continuum damage mechanics framework, where damage evolution (i.e. nucleation and growth of micro-cracks) represents the reduction in the load-bearing capacity of the material. Switching from the continuum description to a micro-mechanical point of view, however, leads to some challenges. First, for both micro-voids and micro-cracks it is difficult to define when damage nucleation actually takes place. The very initial stages of crack nucleation involve events at the atomic scale, which are not possible to be resolved microscopically in full detail. But the challenge goes deeper than this experimental limitation. Even if there could be tools with high enough resolution, the identification of the point of damage initiation would be challenging since both dislocation plasticity and damage involve breaking of some atomic bonds and the transition in

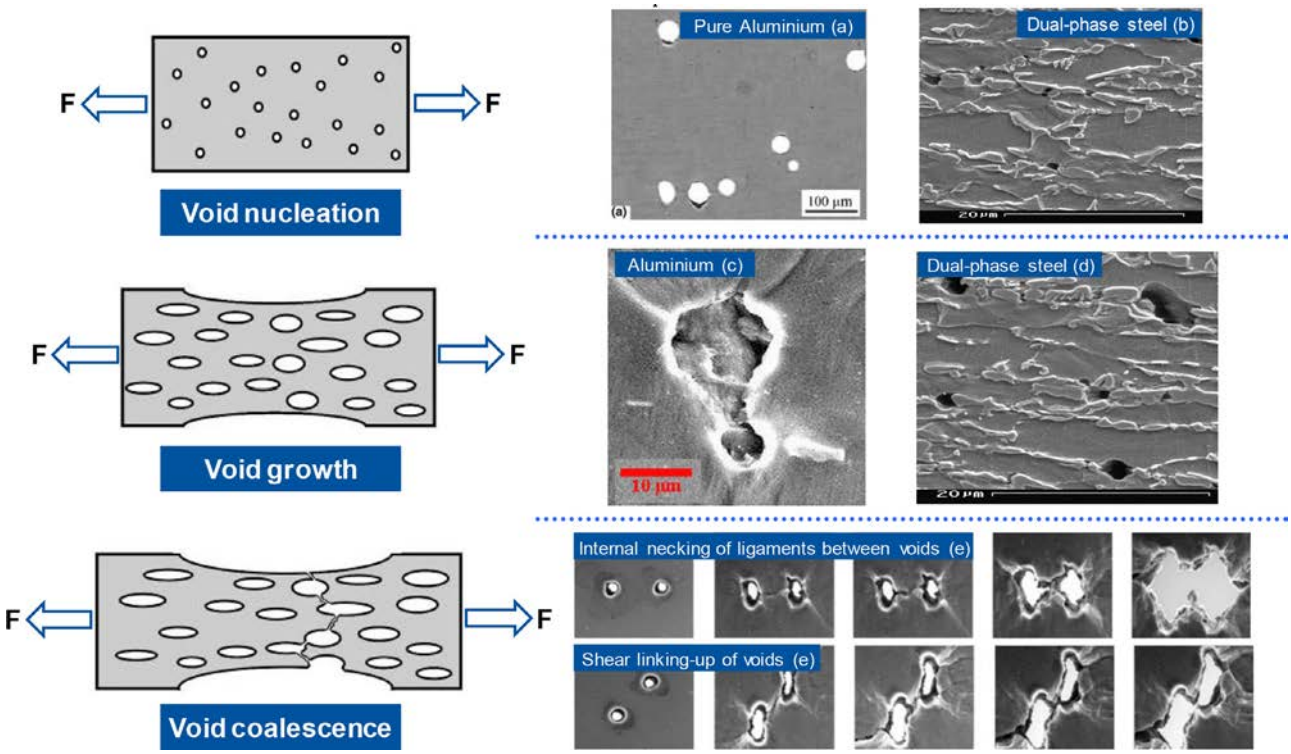

Fig. 3. The illustration of the void-based ductile damage mechanism. (a) The void nucleation by the debonding of the inclusion from the aluminium matrix [10]; (b) The void nucleation by the ferrite-martensite decohesion and martensite cracking in a dual-phase steel [118]; (c) The void growth in an aluminium alloy AA6061T6 [67](d) The void growth in dual-phase steel [118]; (e) The void coalescence by two different mechanisms: internal necking and shearing [215].

between is not necessarily sharp. Stresses developing in a dislocation pile-up can eventually lead to nucleation of a crack. Yet, should the developing local stress effects also be considered as a part of the nucleation process?

Secondly, there are microstructural changes other than formation of micro-voids or -cracks that can create a reduction in the load-bearing capacity of metals. Thermally-induced phase transformations of brittle phases [175], hydrogen uptake and segregation-induced damage sensitivity [146,115], and radiation-induced point defect formation [223,154] are some examples. Some of those effects can also be activated during forming operations, creating further ambiguity on what to call damage. One generic solution is to revert back to the broad definition made above, to apply it to metal forming: any local crystallographic or compositional change in metal substructure, leading to a reduction in the load-bearing capacity of the material, can be referred to as damage. This includes volumetric as well as surface damage. Damage as defined above might affect also other properties of the component such as electro-magnetic, acoustic etc. Here, in the remainder of this text the classical continuum damage mechanics-based description of damage will be employed.

It is often assumed that the coalescence of voids defines the beginning of macroscopic failure and that crack propagation is a series of void coalescences occurring in the structure until complete fracture [2]. Therefore, the discussion of damage in this section is closely related to failure by fracture since the strain at fracture seems to be a quantitative measure of the accumulated damage during plastic deformation. This mechanism is basically valid for most metals and is detailed in the following subsections with focus on typical metal forming metals. For the instability-based mechanism voids are, however, either not evident or decisive for damage.

A comprehensive review of the ductile damage mechanisms for engineering materials is given in [60], emphasizing the interplay between mechanics and microstructural aspects, in [119], discussing the mechanisms of damage for high temperature creep and cold/warm/superplastic metal forming, and in [160] giving an overarching review of the mechanisms and modeling of brittle and ductile fracture.

2.1. Void nucleation

The nucleation of voids is usually associated with strain incompatibility and stress concentration due to the heterogeneous features of microstructures. Interfaces where two microstructural constituents with different mechanical properties meet and merge feature a strong microstructure inhomogeneity leading to favorable sites for void nucleation. These interfaces typically include phase boundaries, grain boundaries, and matrix-particle boundaries. Several experimental studies provide a strong indication for the fracture strain (ductility) of various metals being directly related to the volume fraction of inclusions that serve as sources for void nucleation. Fig. 4 is an example for various copper alloys with different contents of inclusions leading to different ductility or failure strains [51].

Basically, voids nucleate by decohesion of the inclusion from the matrix or by cracking the inclusion. The key parameters for these two types of void nucleation are given in Table 1 by [19].

The influence of the strength of the matrix is investigated by Babout et al. [10] for various aluminum metal matrix composites reinforced by 4% volume fraction of ZrO_2/SiO_2 spherical particles (Fig. 5). X-ray tomography images are obtained during in-situ tensile tests.

In a soft matrix, void nucleation predominately occurs by particle decohesion. The mechanism is also confirmed by McVeigh et al. who modelled 4340 steel under shear-loading conditions, noting that voids nucleate through the decohesion of TiC secondary particles [137]. However, in a hard matrix void nucleation predominately occurs by cracking second phase particles, inclusions, and precipitates. Studies of Shabrov et al. on notched tensile bars of titanium-modified 4330 steel show that voids leading to ductile fracture nucleate from cracking of TiN [180]. The cracking may be viewed as a cleavage process when the local plasticity of these crack triggers is

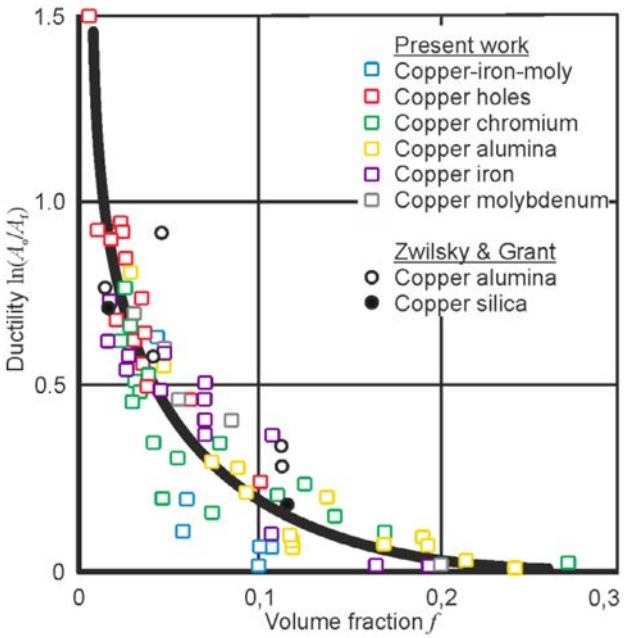

Fig. 4. Correlation of volume fraction of inclusions and voids on the ductility of various copper alloys [51].

Table 1
Key parameters for void nucleation and relative trends upon increasing the parameter for the microscopic mechanism [19].

Parameter	Type	Trend	
		Decohesion	Cracking
Matrix yield strength		↘	↗
Matrix hardening exponent		↘	↗
Particle elongation		↘	↗
Particle stiffness		↗	↗
Load orientation	Axial	↘	↗
	Transverse	↗	↘
Load triaxiality		↗	↘

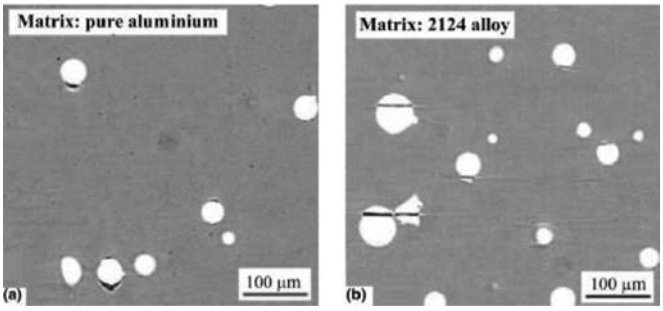

Fig. 5. Different void nucleation mechanisms for (a) a soft aluminium matrix and (b) a hard aluminium matrix [10].

limited or inexistent [102]. This mechanism is found in many multiple-phase steels where the void nucleation occurs in the brittle phases, such as martensites [191,104].

For modern high-strength steels with complex microstructures, the competition of these mechanisms is evident and the interrelation of them is strongly dependent on the microstructural features. For example, the major mechanisms of void nucleation of dual-phase steels are martensite cracking, ferrite–martensite interface decohesion, and ferrite–ferrite grain boundary decohesion. The dominant damage mechanisms are controlled by the morphology (size, shape, and distribution) of the martensite phase, its volume fraction, the ratio of the yield stress of the ferrite to the martensite phase, and, finally, the chemical composition [203]. For dual-phase steels with low or intermediate martensite volume fraction, Ahmad et al. [3] showed that mainly ferrite–martensite interface decohesion is the

void initiation mode, while the ferrite–ferrite interface decohesion and martensite cracking are more dominant for high-volume fraction of the martensite phase. Martensite cracking, on the other hand, can be promoted through the morphology of the coarse and interconnected martensite along the ferrite grain boundaries [53]. The main damage mechanism in dual-phase steels with coarse grains is martensite cracking, whereas for DP-steels with ultra-fine grains ferrite-martensite interface decohesion is the primary damage mechanism [33].

The evolution of void nucleation under shear loading has been investigated for a High-Strength Low-Alloy Steel (HSLA) by Achouri et al. [1] based on in-situ tests. In their test for shear-dominant parts of the specimen voids nucleate by debonding (Fig. 6).

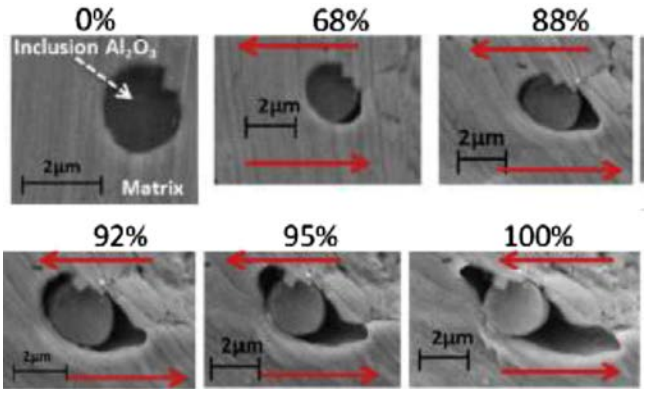

Fig. 6. Void nucleation by debonding for various shear loadings expressed as proportions of displacement at fracture for a HSLA steel [1].

Depending on the stress state and material hardening, also fracture of inclusions or a mixture of debonding and fracture have been observed. The various void mechanisms of void formation under tension and void formation by shear can be related to the stress triaxiality as given in Fig. 7 [30].

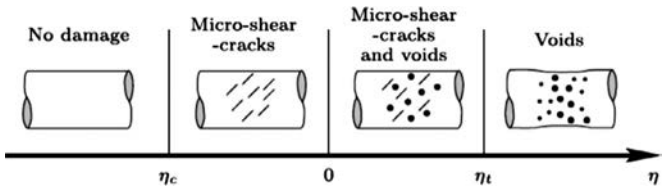

Fig. 7. Different damage mechanisms depending on stress triaxiality [30]. η_c is the stress triaxiality at simple compression and η_t at simple tension.

2.2. Void growth

After void nucleation, both void growth and distortion could take place. Different from the void nucleation mechanisms that are mainly dependent on the intrinsic features of the microstructure, the decisive factors for either void growth or distortion are extrinsic, e.g. the stress states. It is commonly accepted that void growth is triggered when the stress triaxiality is large [61]. The first micromechanical models developed by McClintock [136] and Rice & Tracey [163] in the late 60's provide an overview of the combined effects of stress triaxiality and plastic strain on ductile void growth. Marino et al. [134] studied the growth of voids at artificially embedded, weakly bonded inclusions to validate the form of the void growth law by Rice and Tracey [163]. Barnby et al. [17] discovered that when the triaxiality value is less than about 1.2, the void growth predicted by Rice-Tracey theory is close to the real void growth rate in C-Mn structural steel. However, when the stress triaxiality is larger than about 1.2, the actual void growth rate in the structural steel is less than the void growth rate determined by the Rice-Tracey model.

The void growth in simple tension of copper has been studied by Weck et al. [215] up to an equivalent plastic strain of twice the value at the beginning of necking. They observed that at the beginning of deformation, the rate of void elongation is about twice the elongation rate of the specimen due to the stress concentration around the void. With further deformation this elongation rate slows down. With necking the triaxiality increases and the voids also grow laterally. Due to plastic flow localization the kinetics of void growth changes substantially.

Gross and Ravi-Chandar [67] observed in-situ the void growth in an Al 6061-T6 alloy under plane strain bending conditions utilizing a scanning electron microscope (SEM), Fig. 8. The area growth in the matrix around the cavity is 35%, while the area growth of the cavity is 260% (from 9.2 to 33.2 μm^2). The voids elongated basically in tension direction. With further plastic deformation the voids even grow by 930% for a matrix deformation of only 210%. The average triaxiality is nearly 0.57.

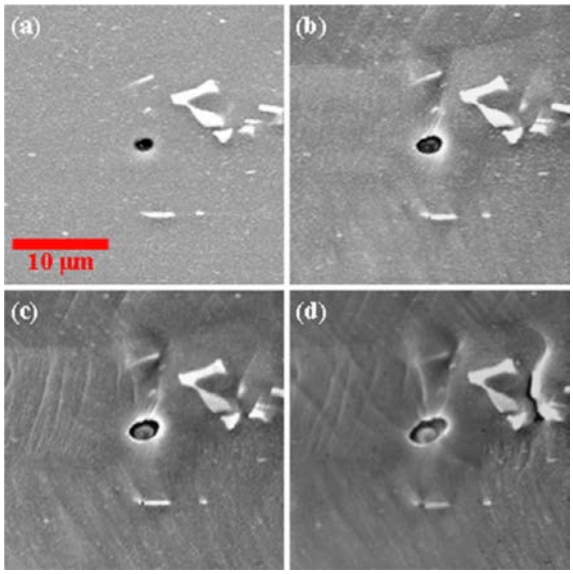

Fig. 8. Evolution of an existing void in Al 6061-T6 under plane strain tension [67]. Bending strain increases from zero (a) to maximum value (d).

2.3. Void distortion

During plastic deformation voids not only change their size, but also their shape. The voids are basically elongated in the loading direction under tensile loading or shear loading. The shape change of artificial voids in a pure copper specimen under tensile loading is investigated in [215]. Pineau et al. [160] state that void shape changes are stronger at low stress triaxiality values and could be critical for the damage level. The type of void distortion depends on the existence of shear stress component and also on the void-inclusion interaction. Fig. 9 shows the evolution of voids under shear loading for a ferrite-bainite steel (FB600) obtained by synchrotron laminography. The voids start to form at particles in the shear direction [165].

2.4. Void coalescence

After void nucleation and growth, voids finally link through an instability in the inter-void ligament and this coalescence of voids leads to final fracture. Void coalescence occurs in a variety of modes, each with multiple variants, depending on microstructure factors, loading conditions, and plastic flow characteristics [215,21]. This phenomenon can be divided into two major modes: internal necking of voids and shearing. This was discussed by Argon et al. [7]. Rui et al. studied the fracture of FeNi42 alloy and observed that coalescence of voids occurs in localized necked regions [57].

For shearing-based void coalescence two different types of shearing shall be distinguished: shearing of the interstitial ligament and void-sheet formation. For the first one the nucleation of voids in a shear band and subsequent elongation of these voids along the shear

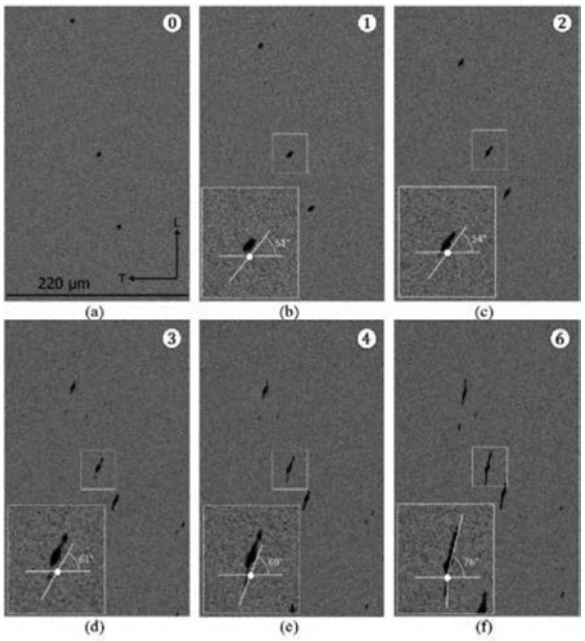

Fig. 9. Development of voids under shear loading in a ferrite-bainite steel (FB600) [165].

band results in inter-void shearing, causing voids to coalesce and create macroscopic cracks in the plane of the shear band [152]. Cox et al. [48] observed in AISI 4340 and nickel-200 grade maraging steel that a ductile crack linking the pre-existing voids is created by void-sheet formation (Fig. 4e) generated through shear localization between existing voids and the nearly simultaneous nucleation and coalescence of new voids in this localization. Jablokov et al. [89] characterized strain-induced void growth and coalescence in HY 100 steel subjected to tensile failure over a range of temperatures (−85 °C to 25 °C), strain rates (10^{-3} to 10^{3} s^{-1}), and stress-states (stress triaxiality of 0.8 to 1.3). Chae et al. showed that for these stress triaxiality conditions the HY-100 fails due to the growth and coalescence of elongated MnS-nucleated voids by the void-sheet mechanism [41]. Both inter-void shearing and void-sheet formation produce ductile cracks that connect multiple voids along a shear band. However, they are two different mechanisms [57]. Void shearing is characterized by nucleation of a few voids and subsequent growth along the shear zone (void growth is rate- limiting), while void-sheet formation is characterized by nucleation of many voids in such close proximity that they coalesce after relatively little growth (void nucleation is rate-limiting). The coalescence of voids is depicted by in-situ laminography for nodular graphite cast iron in Fig. 10 [31].

The comprehensive study on the effect of matrix strength on the void behavior under plastic strain for aluminium matrix by Babout et al.

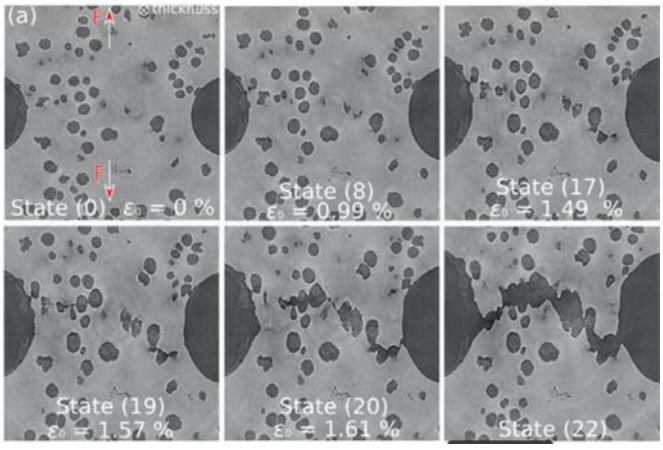

Fig. 10. Coalescence of voids for graphite cast iron during plastic deformation [31].

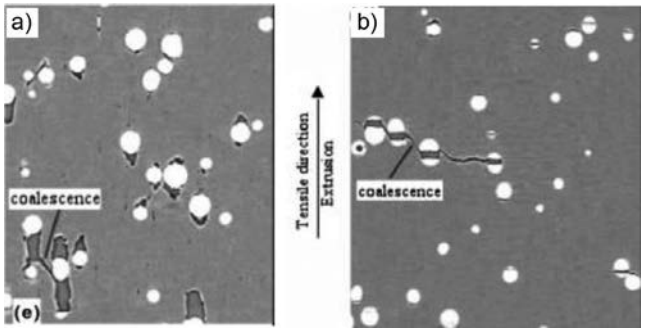

Fig. 11. Coalescence of voids for a soft aluminium matrix (a) with equivalent plastic strain of about 0.6 and for a hard aluminium matrix (b) with equivalent plastic strain of about 0.15 [11].

[11] shows in Fig. 11 that for the hard matrix the coalescence of voids takes place over much larger distances than in the case of a soft matrix.

3. Characterization of damage micro-mechanisms

Damage nucleation is a consequence of critical changes in microstructure, stress and strain fields. An improved understanding of these mechanisms, thus, requires development of experimental tools that are capable to map these different fields and how they evolve. In this section current tools and trends in experimental methods for characterizing microstructural damage in metallic materials will be reviewed. Here, the focus is mostly on ductile damage. The discussed characterization methods are also often relevant for damage mechanisms triggered under different deformation boundary conditions (e.g. damage due to fatigue, creep, wear, etc.). It should also be noted that damage characterization efforts can be grouped into two based on the underlying goal: characterization of damage micro-mechanisms and quantification of damage evolution. The former is focused on unraveling the physical nature of damage evolution – a goal of most specific interest to the fields of mechanical and physical metallurgy and is discussed in this section. The latter is focused on quantifying the relationship between deformation and damage – a goal of interest to the fields of computational and continuum (damage) mechanics and is discussed in Section 4.5 since it is closely related to the modeling of damage. These two groups have some overlaps in the techniques employed.

Due to the engineering importance of metal failures, mechanisms of void nucleation, growth, and coalescence have been of interest for decades, mostly to guide alloy and micro-structure design efforts (for Bainite [148], for Al6xxx [107], TRIP-assisted multiphase steel [90], correlating the fracture surface [133]), but also to develop models with predictive capabilities as described in Section 4 in detail. From an experimental perspective, most classical studies of fracture rely on SEM-based fracture surface investigations to understand failure mechanisms [9,94]. However, most such analyses are qualitative in nature, as demonstrated in identifying the role of interlath austenite on hydrogen-embrittlement resistance of martensitic steels [211], or of strain-path effects on damage mechanisms in interstitial-free and dual-phase steels [190]. There are also more analytical investigations of fracture surface features. For example, Hong and Laird investigated fracture surfaces of fatigued Cu-16Al single crystals (Fig. 12a) [83]. Their fracture surface topography and slip trace analyses revealed that the cross-slip plane is the most favored slip system for linking up parallel primary cracks in this alloy

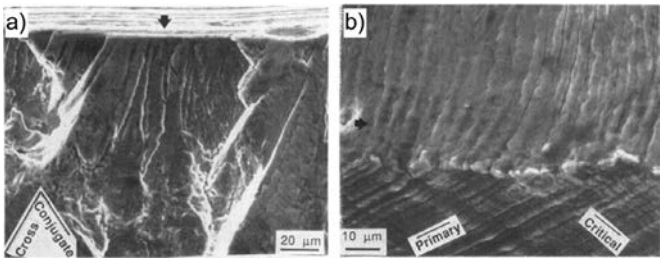

Fig. 12. (a) Fatigue crack initiation location and (b) striation marks in a Cu-Al alloy [83].

(Fig. 12b). Martin et al. demonstrated some of the strongest evidence for the hydrogen-enhanced localized plasticity theory through a combined SEM, a focused ion beam (FIB), and a transmission electron microscopy (TEM) study of fracture surfaces in steels [135].

Fracture surface investigations provide only a snapshot of the final stage of deformation. Most structural metals, however, are ductile and they have damage-prone multi-phase microstructures which exhibit damage nucleation already at low strain levels, e.g. immediately after yielding. Thus, to better understand damage mechanisms, microstructure investigations of samples deformed to different levels of deformation are carried out, typically utilizing SEM-based techniques in a post-mortem manner. A common motivation for carrying out such analyses is to assess the competition between micro-cracking and decohesion mechanisms, for example in dual-phase steels [191]. Hoefnagels et al. demonstrated that the activity of these two damage mechanisms is influenced not only by the microstructure, but also by the strain path [82] (Fig. 13).

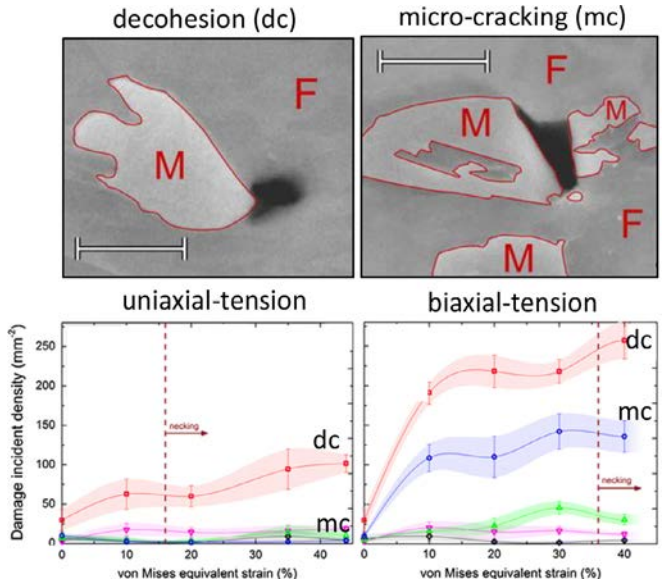

Fig. 13. Martensite-ferrite decohesion (dc) and martensite micro-cracking (mc) mechanisms in dual phase steels (above). Upon switching from uniaxial tension to biaxial tension both mechanisms become more active (below) [82]. The scale bar indicates a length of 1 μm.

The 2D nature of SEM-based methods and the resulting necessity for sample preparation create some challenges. Systematic investigations show that mechanical polishing methods may reveal underestimated damage contents (due to smearing effects), and chemical- or electro-chemical methods may cause overestimates of damage content (due to pitting effects) [194]. To overcome preparation challenges, Isik et al. prepared specimens extracted from a tensile test sample by ion-slope cutting (Fig. 14), which enabled investigations of voids sub-100 nm in diameter [86].

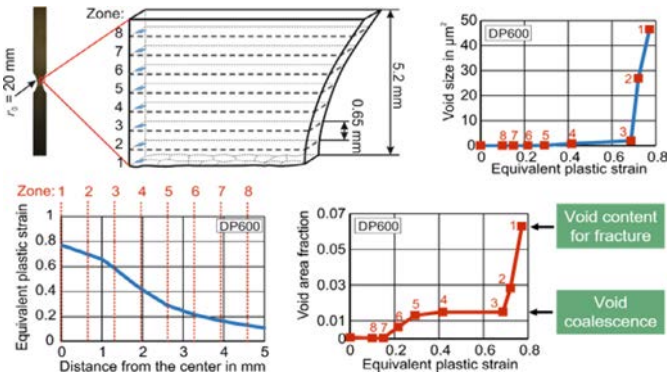

Fig. 14. Evolution of void size and void area fraction in DP600 during a tensile test with a notch [86].

To overcome challenges associated with the 2D nature of electron microscopy, X-ray micro-tomography based techniques have been employed routinely, often together with in-situ deformation, to gather deformation and damage data from the bulk [194,132]. Despite limitations in spatial resolution, which mean that damage nucleation mechanisms are harder to observe, the 3D data produced are extremely rich, especially with regard to damage growth and coalescence mechanisms, for example in dual phase steels [131] or high carbon steels [37]. For thin sheets X-ray laminography, overcoming the restriction of axisymmetric specimens, is successfully applied in [149].

Another limitation of the X-ray micro-tomography, as well as other techniques, concerns the coupling of microstructure and strain mapping to damage mapping. Advanced alloys typically have mechanically-contrasting phases in their microstructure, leading to micro-scale strain-stress localization prior to damage phenomena [189,192]. In many cases, spatial variations in composition (which may be influenced by deformation [196,73]) play a role [101] as well. Thus, unraveling the full complexity of damage mechanisms requires more than simple imaging of cracks. There is a great interest to develop in-situ experimental methods that would allow multi-field mapping, i.e. simultaneous mapping of mechanical and microstructural fields.

A synchrotron-based approach that overcomes the challenge of mapping microstructure and damage is developed by Toda et al., which utilizes phase- and absorption-based tomography together [202,201]. Also, several analytical mapping techniques are becoming standard in SEMs, providing contributions to the understanding of damage mechanisms, even when applied post-mortem. For example, León-García et al. have identified how TiN particles in interstitial-free steels induce damage through particle fragmentation, particle–matrix debonding, and void growth by using electron backscatter diffraction (EBSD) to capture matrix rotations (Fig. 15) [114]. Koyama et al. used electron channeling contrast imaging (ECCI) to demonstrate hydrogen damage in lightweight steels. More specifically, the researchers examined dislocation slip localization leading to grain boundary cracking, using ECCI [100].

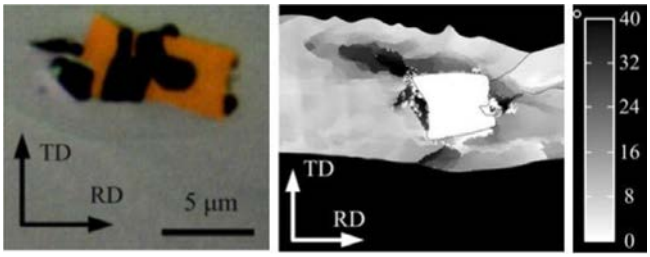

Fig. 15. TiN particle in an interstitial-free steel exhibiting both decohesion and particle cracking mechanisms (left) which induce crystal rotations in degree (right) [114].

Recent trends in metals design also include the reduction of phase stability [117,52], often aiming for fine-structured, multi-phase, metastable microstructures. Such materials evolve in multiple ways with deformation; thus, their analysis requires in-situ approaches. In-situ experiments in the SEM enable the use of digital image correlation (DIC), EBSD, and ECCI in an integrated manner [189,218]. An example is shown in Fig. 16, where Wang et al. have demonstrated that martensite size effects play a key role in strain localization and damage nucleation in quench and partitioning steels [212]. One current limitation of the 2D SEM-based DIC technique is the absence of strain measurement along the normal direction to the observed surface. A promising method for enabling 3D analyses of strain is the combination of X-ray laminography and digital volume correlation (DVC) [31].

4. Modeling damage

The modeling of damage in bulk metal forming processes is based on either uncoupled fracture criteria or coupled damage models, both built on micromechanical or phenomenological bases. In the first family the damage variable does not interact with the material behavior, whereas in the second one damage is coupled with elastic

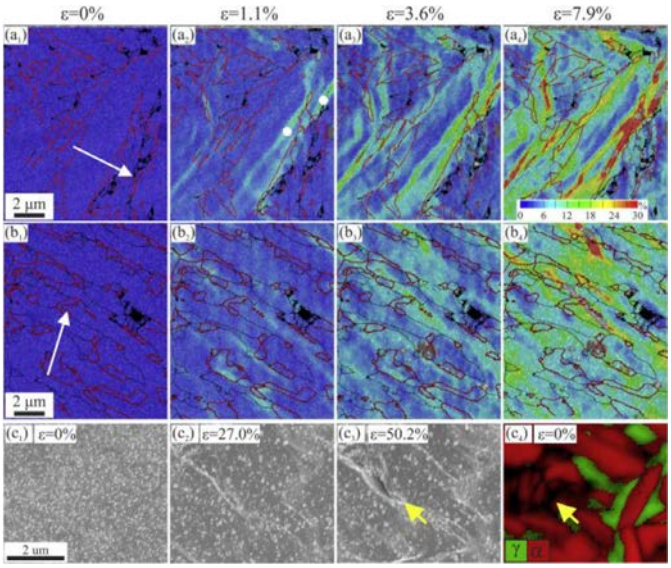

Fig. 16. Evolution of the local strain as a function of the martensite matrix with (a) coarser and (b) finer substructure in a QP steel, (c) microstructure [212].

and/or plastic material behavior. This last family is split into phenomenological damage models and micromechanical ones that enable to predict the material's damage-based softening effect (see Fig. 17).

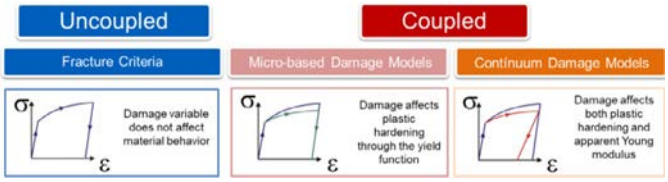

Fig. 17. The three main approaches for modeling damage and their influence on the material behavior.

Regarding sheet metal forming, conventional forming limit curves (FLCs) are still used in the industry to predict necking failure. However, this method is not appropriate to address damage issues and also fails when predicting fracture for many industrial applications exhibiting non-linear strain paths. Though some attempts were made to determine FLCs using conventional coupled damage models [97], this paper will not address FLCs in the following.

This section focuses on the most commonly used ductile damage models. It is followed by details about the particularity of damage related to material forming applications and by indications about model's calibration. Finally, the last subsection aims to provide guidance for the selection of an appropriate model for a particular application?

For more details readers can refer to more general reviews dedicated to ductile fracture: starting with a review from the 2000s [119] and a more specific summary dedicated to modeling in the 2010s [23] continuing with a general and broad overview of ductile fracture [19] and, finally, the most recent one on modeling in cold forming [38].

Before describing the damage models, the commonly used stress state parameters are defined: The normalized stress state can be represented by two independent parameters, i.e. the stress triaxiality η and the Lode parameter L. The stress triaxiality is defined as

$$\eta = \frac{I_1}{3 \cdot \sqrt{3 \cdot J_2}} = \frac{\sigma_h}{\sigma_{vM}}, \tag{1}$$

with I_1 and J_2 denoting the first invariant of the stress tensor and the second invariant of the corresponding deviatoric stress tensor that are related to the hydrostatic stress σ_h as well as the equivalent von Mises stress σ_{vM}, respectively. This parameter controls physically the size of the void. Lode [122] defined the Lode parameter as

$$L = \frac{2\sigma_2 - \sigma_1 - \sigma_3}{\sigma_1 - \sigma_3}, \text{ with } L \in [-1, 1]. \tag{2}$$

where σ_1 to σ_3 are the principal normal stresses. This parameter controls physical the shape of the void. In literature, the Lode angle θ and the normalized Lode angle $\bar{\theta}$, also known as Lode angle parameter, are widely used. The relation between the Lode parameter and the normalized Lode angle can be approximated by $\bar{\theta} \cong -L$. The exact transformations are given in [125]. The Lode angle is denoted as

$$\theta = \frac{1}{3} \arccos\left(\frac{27 \det(\boldsymbol{\sigma}^{dev})}{2\, \sigma_{vM}^3}\right), \text{ with } \theta \in [0, \pi/3\ ], \tag{3}$$

where the determinant of the deviatoric stress tensor is defined as its third invariant J_3. The normalized Lode angle can be obtained with the following transformation:

$$\bar{\theta} = 1 - \frac{6 \cdot \theta}{\pi}, \text{ with } \bar{\theta} \in [-1, 1]. \tag{4}$$

4.1. Failure criteria

One of the first criteria was proposed by Freudenthal and Geiringer [56]. They suggested that failure occurs once the generalized plastic work reaches a critical value. This pioneering work was followed by many other criteria where a damage variable D was defined as the integral of a stress function $\omega(\sigma)$ over the plastic strain ($\bar{\varepsilon}_p$) path. Failure occurs when D reaches its critical value (D_c) for a given strain to fracture $\bar{\varepsilon}_f$:

$$D = \int_0^{\bar{\varepsilon}_f} \omega(\boldsymbol{\sigma}) d\bar{\varepsilon}_p \tag{5}$$

Based on micromechanical or phenomenological assumptions, the first criteria accounted for either the maximum principal stress [47], the maximum stress weighted by the mean stress [27], or the stress triaxiality η [163] and sometimes the hardening coefficient [136]. These criteria were popular since the only parameter to identify was the critical damage value. They are still used a lot in the industry because of their simplicity. Their prediction for complex loading paths is questionable because the critical damage value depends on the loading path and, hence, they should be used only in a qualitative manner.

More recently, Bao and Wierzbicki showed that stress triaxiality should be completed by the Lode angle θ (or normalized Lode angle $\bar{\theta}$ or Lode parameter L) in order to define the normalized stress state in a unique way [14], see also Eqs. (1) and (2). They showed that the Lode angle influenced ductile fracture, in particular for low stress triaxiality values. Many other criteria accounting for both stress triaxiality values and Lode angle followed. These criteria usually define a fracture locus where the strain to fracture is a function of stress triaxiality and Lode angle [12].

The integral form of these criteria can be written as follows:

$$D = \int_0^{\bar{\varepsilon}_f} \frac{1}{\bar{\varepsilon}_f(\eta, \bar{\theta})} d\bar{\varepsilon}_p \tag{6}$$

$\bar{\varepsilon}_f(\eta, \bar{\theta})$ stands for fracture strain only for proportional loading conditions, [36]. Under these conditions, failure occurs when D equals 1. For non-proportional loading conditions some authors [12] suggest to use the average stress history for η and $\bar{\theta}$. This approach, however, was invalidated by Benzerga et al. [20] based on unit-cell coalescence analyses for non-proportional loading paths. Using the final stress values at the onset of fracture would also be inaccurate since it does not account for the history of the loading path. For such failure criteria $\bar{\varepsilon}_f$ should therefore be seen as a weighting function depending on the stress path, i.e. the strain at the onset of fracture for a loading path characterized by a stress state history during plastic loading defined by $\eta(\bar{\varepsilon}_f)$ and $\bar{\theta}(\bar{\varepsilon}_f)$.

There are so many fracture criteria in the literature that it is difficult to select the most appropriate. Among all these criteria, it is worth mentioning the modified Mohr-Coulomb (MMC) criterion,

initially proposed by Bai and Wierzbicki [12] and extended by Mohr and Marcadet who showed good prediction on three advanced high-strength steel sheets (DP590, DP780 and TRIP780) [145]. Lou and co-workers also defined an interesting fracture criterion as the multiplication of three terms acting for nucleation, growth, and coalescence mechanisms [124]. This criterions was extended to account for Lode dependency and a stress triaxiality cut-off value was added [125]. The latest version of the model ([123]) showed good results for an AA6082 T6 aluminium alloy under sheet metal forming conditions. According to the authors this criterion can also be used to predict the onset of failure for bulk metal forming provided that the parameters are calibrated using representative stress state conditions.

Failure criteria are very popular in the metal forming community. This popularity is due to their relatively simple implementation in any finite element code. The fact that they are not coupled to the material behavior preserves them from any convergence issue. They are consequently not sensitive to mesh-dependency coming from damage localization issues (see next section). They also facilitate the comparison between different criteria since they can be used and compared all together in a post-processing stage. The main drawback of these criteria lies in their incapability of modeling material softening due to damage growth and their questionable accuracy for non-proportional loading paths.

4.2. Phenomenological damage models

Built on thermodynamical assumptions, the so-called continuum damage models (CDM) are based on the initial framework defined by Kachanov [96]. But these models became really popular after the work of Chaboche [40] and Lemaitre [111]. They rely on a thermodynamic framework which guarantees that dissipation remains always positive. The damage variable (D) is considered as an internal scalar variable which, for a given internal surface of normal $\vec{n}$, stands for the ratio of the damaged area A_D to the total surface A of the cross section (Fig. 18):

$$D = A_D/A \; (0 \leq D < 1) \tag{7}$$

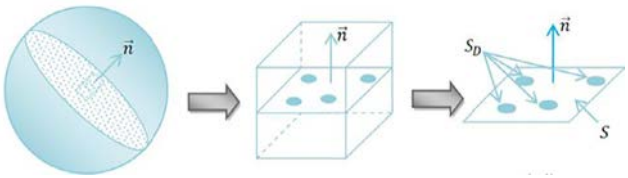

Fig. 18. Representation of damaged area for the definition of damage variable D.

The damage evolution law is defined by:

$$\dot{D} = \dot{\lambda}\frac{\partial F_D}{\partial Y} = \dot{\bar{\varepsilon}}_p\left(\frac{Y}{S}\right)^b, \tag{8}$$

where $\dot{\lambda}$ is the plastic multiplier, S and b are Lemaitre damage parameters and Y, the energy density release rate, is the variable associated with D and is derived from the state damage dissipation potential F_D [111]:

$$Y = \frac{\bar{\sigma}^2}{2E(1-D)^2}\left[\frac{2}{3}(1+\nu) + 3(1-2\nu)\eta^2\right], \tag{9}$$

$$F_D = \frac{S}{(1+b)(1-D)}\left(\frac{Y}{S}\right)^{b+1}, \tag{10}$$

with ν being the Poisson's ratio and E the apparent Young's modulus.

In order to account for damage in the macroscopic behavior, the effective stress $\tilde{\sigma}$ is defined based on the strain equivalence principle. $\tilde{\sigma}$ defines the stress that should be applied to an undamaged material in order to get the same strain tensor as the one obtained from the damaged material under actual stress:

$$\tilde{\sigma}_{ij} = \sigma_{ij}/(1-D). \tag{11}$$

Therefore, this effective stress enables to couple damage evolution with the material behavior law. As observed experimentally, damage also affects elasticity and the apparent modulus of damaged elasticity ($\tilde{E}$) can be defined using the damage variable by:

$$\tilde{E} = E(1-D). \tag{12}$$

This model is therefore able to account for the effect of damage on both elasticity and plasticity.

Based on this initial framework, various contributions were developed in order to improve damage prediction with this model regarding material forming processes. It is, for example, possible to define a strain threshold (ε_D) below which damage does not increase [112]. Chow and Wang were the first to propose a generalization of the Lemaitre damage model to anisotropic damage [43] and the detailed tensor framework is available in [112]. Damage anisotropy often comes from material flow during bulk forming and Bouchard et al. account for the influence of grain flow orientation on anisotropic ductile damage [25].

A particularity of metal forming is also the complexity of the loading path. For non-proportional loading conditions voids that nucleated during positive stress triaxiality conditions can then be subjected to compressive loading stress states. Thus, voids can close so that the material recovers, at least partially, its initial properties, which needs to be accounted for in the energy density release rate. Quasi-unilateral conditions of micro-defects closure were initially proposed by Ladevèze and Lemaitre [109] and their positive influence on the prediction of fracture in metal forming [6] was shown by Andrade Pires et al. in bulk metal forming and Bouchard et al. for upsetting, extrusion, and tensile tests [25]. The cut-off value for very low stress triaxiality [15] was also added in a Lemaitre model by Bouchard et al. [25], whereas Chow and Wei proposed and applied a tensorial extension to model cyclic loading in an aluminum alloy [44]. Pirondi and Bonora investigated the extension of the Lemaitre model to account for cyclic loading in SA 537 steel [161]. Such cyclic loading conditions may occur during incremental forming processes such as Mannesmann or flow forming processes.

By definition of the energy density release rate, damage growth is essentially a function of stress triaxiality and equivalent stress. In order to account for the effect of Lode angle, a Lode-dependent Enhanced Lemaitre model (LEL) was defined by Cao et al. in [35]. This extension also includes a stress-triaxiality dependent strain damage threshold (ε_D) and an enhanced weakening function to account for the influence of damage on the material behavior at low stress triaxiality.

If the Lemaitre damage model is the most commonly used phenomenological model, it is worth mentioning three additional interesting approaches:

- In the Rousselier damage model [166] the yield surface is modified to account for porosity, which is the damage state variable.
- The CDM thermodynamically consistent framework developed by Brünig which relies on a kinematic description of damage leading to the definition of damage strain tensors [28]. A multiplicative decomposition of the strain tensor is defined and includes, in addition to an initial damage term, the elastic deformation of the material body, the plastic deformation of the fictitious undamaged body as well as the deformation induced by damage accumulation.
- The Generalized Incremental Stress State Dependent Damage Model (GISSMO) defines a scalar damage variable (D) as well as an instability measure (F) which is a function of the critical strain $\varepsilon_{crit}(\eta)$. When this variable F, which can be interpreted as an instability criterion, reaches 1 the coupling between the damage variable and the stress tensor is activated [5].

Continuum damage models enable to account for the softening effect due to damage accumulation that makes them very valuable for metal forming applications and subsequent studies on mechanical strength of formed components. Another advantage of these models compared to micromechanical approaches (see next section) is their relatively low number of damage parameters as well as their ability to couple damage with elasticity. However, the softening effect in both micromechanical and continuum damage mechanics models is known to induce mesh dependency through the so-called *damage*

localization phenomenon. This results in faster damage accumulation for finer meshes [92]. Such mesh dependency can be overcome by using non-local approaches based either on integral formulations [18] or implicit/explicit gradient formulations [158]. A more detailed overview is given in [159]. A non-local implicit gradient formulation was used in [39] to model external tube inversions and sheet blanking processes. The main issue with such non-local approaches is the definition of the characteristic length used for the regularization which has to be larger than the mesh size.

4.3. Micromechanical damage models

Ductile damage (at least for positive stress triaxiality conditions) relies on the nucleation, growth and coalescence of micro-voids. After the former work of Rice and Tracey [163] and Mc Clintock [136] the first attempt to take into account the effect of void growth on material behavior was proposed by Gurson who developed an upper bound analysis for a finite sphere containing a spherical void and for a rigid perfectly plastic matrix [68]. Tvergaard and Needleman extended this theory to plastic hardening material and defined the well-known Gurson-Tvergaard-Needleman (GTN) model [208]. In this porous plasticity theory, the yield function Φ is defined by:

$$\Phi = \left(\frac{\overline{\sigma}}{\sigma_0}\right)^2 + 2q_1 f^* \cosh\left(-\frac{3}{2}q_2\frac{p}{\sigma_0}\right) - 1 - q_3 f^{*2}, \tag{13}$$

where $\overline{\sigma}$ and σ_0 are the equivalent stress and the flow stress, respectively, p is the hydrostatic pressure, q_1, q_2 and $q_3 = q_1^2$ material constants. In addition, f^* is the effective void volume fraction that accounts for void coalescence according to:

$$\begin{cases} f & \text{for } f \le f_c \\ f_c + \dfrac{f_u^* - f_c}{f_f - f_c}(f - f_c) & \text{for } f_c \le f \le f_f \end{cases}, \tag{14}$$

where f is the void volume fraction, f_c the void coalescence threshold, f_f the void volume fraction at fracture and f_u^* the effective void volume fraction at fracture.

The evolution of the void volume fraction is driven by a nucleation and a growth contribution:

$$\dot{f} = \dot{f}_{\text{nucleation}} + \dot{f}_{\text{growth}}, \tag{15}$$

where growth depends on the trace of the plastic strain rate:

$$\dot{f}_{\text{growth}} = (1-f)\,\text{tr}(\dot{\varepsilon}_p). \tag{16}$$

The most common nucleation function is the one proposed by Chu and Needleman with strain-controlled and stress-controlled terms [45]:

$$\dot{f}_{\text{nucleation}} = A\dot{\bar{\varepsilon}}_p + B(\dot{\overline{\sigma}} + c\dot{p}), \tag{17}$$

where A and B are functions of $\bar{\varepsilon}_p$ and $\overline{\sigma} + cp$, respectively, and follow a normal distribution such as:

$$A(\bar{\varepsilon}_p) = \frac{f_N}{S_N\sqrt{2\pi}}\exp\left[-\frac{1}{2}\left(\frac{\bar{\varepsilon}_p - \varepsilon_N}{S_N}\right)^2\right], \tag{18}$$

with ε_N being the mean value of the plastic strain at maximal nucleation, S_N the standard deviation of Gaussian distribution corresponding, and f_N the total void volume fraction that can be nucleated.

It must be noted that, in literature, the second term of the nucleation evolution law, Eq. (17), is not always taken into account. The nucleation stress dependency may then be added directly in the term ε_N that can depend on stress triaxiality as detailed in [37].

This model became very popular thanks to its micromechanical bases and multiple extensions were proposed in the literature. Gologanu, Leblond, and Devaux were the first to extend the theory to account for void shape change [64] with a recent generalization to arbitrary ellipsoidal voids [130]. Plastic anisotropy, kinematic hardening, void-particle interaction as well as enhanced coalescence formulation were studied in [19] and applied to cold bulk metal forming [38].

Regarding metal forming applications, one of the main drawbacks of GTN approaches was its inability to model ductile failure under shear conditions (because of the void volume fraction growth rate definition). To address low stress triaxiality applications, Xue [217] and Nahshon and Hutchinson [150] decided to add a stress-dependent extra term (accounting for the Lode angle) in this void growth. This is, however, a phenomenological extension of the model. More recently, Jiang et al. used two distinctive damage parameters in the yield function, one related to the void growth mechanism (f^*) and one to the void shear mechanism (D_{shear}) [91]. For this last damage parameter, similarly to the CDM effective stress concept, they defined effective equivalent and hydrostatic stresses which account for D_{shear}. The new yield function Φ is defined by:

$$\Phi = \left(\frac{\overline{\sigma}}{\sigma_0(1-D_{\text{shear}})}\right)^2 + 2q_1 f^* \cosh\left(-\frac{3}{2}q_2\frac{p}{\sigma_0(1-D_{\text{shear}})}\right) - 1 - q_3 f^{*2} \tag{19}$$

These micromechanical models also suffer from mesh dependency and should be associated with non-local approaches. Despite recent phenomenological improvements, GTN approaches are often considered favorably in the literature thanks to the fact that void volume fraction can be measured experimentally. However, due to their large number of parameters, including micromechanical parameters, the calibration process is often heavier. In addition, contrary to Lemaitre-based damage models, elasticity is not coupled with damage evolution.

4.4. Specificity of metal forming

Metal forming induces complex loading paths. If stress states as well as non-proportional loading conditions were discussed above, the influence of strain rate and temperature on the material's ductility and, consequently, on damage prediction must also be considered. Before addressing damage analyses, it is worth mentioning that whatever damage model used, an accurate ductile fracture prediction is only possible if the elastic-viscoplastic behavior is identified properly. Indeed, metal forming often involves local high strain rates which give rise to both increased hardening and self-heating induced softening. It is therefore essential for the material behavior law to be identified properly for the range of strain rate and temperature encountered in the process.

Separating the effects of strain rate and temperature increase requires the use of both local DIC and temperature measurements. If this is not possible, then only the effect of loading velocity can be studied. This is what was done in [50] for a TRIP780 steel sheet where it was shown that strain to fracture indeed increases for higher loading velocity. It is interesting to notice that for a given applied velocity, the equivalent local plastic strain rate at the onset of fracture can be 20 times higher than its value prior to localized necking. In [164], an increased strain to fracture was observed when increasing the strain rate (from 0.001 s^{-1} to 1000 s^{-1}) for a DP590 steel. A rate-dependent Hosford-Coulomb fracture initiation criterion was defined based on an analogy with the Johnson-Cook fracture criterion [93]. In the latter, the strain rate dependency as well as the temperature dependency are added in a phenomenological way, which leads to a strain to fracture defined by:

$$\overline{\varepsilon}_f = [C_1 + C_2\exp(C_3\eta)]\left[1 + C_4\ln\left(\frac{\dot{\bar{\varepsilon}}_p}{\dot{\varepsilon}_0}\right)\right][1 + C_5 T^*], \tag{22}$$

where C_1 to C_5 are damage parameters, $\dot{\varepsilon}_0$ is the reference strain rate, and T^*, the homologous temperature, is defined by:

$$T^* = \frac{T - T_{\text{room}}}{T_{\text{melt}} - T_{\text{room}}} \tag{23}$$

T_{room} and T_{melt} are room and melting temperatures, respectively. Any fracture criterion could therefore be extended in the same way to account for both strain rate and temperature dependence. This is what Liu et al. [121] did to extend the Bao-Wierzbicki fracture criterion with application to metal cutting processes.

Beside its influence on the material behavior, an elevated temperature can also lead to microstructural evolution which, in turn, influences ductile fracture occurrence. In addition, when temperature increases, the matrix behavior tends to soften, leading to lower stresses at interfaces with particles which tend to delay void nucleation. Addressing such microstructure dependency is really complex

and authors usually study the influence of temperature on ductility in a phenomenological way. Valoppi et al. [209] also extended the Johnson-Cook failure criterion. Their application, dedicated to Ti6Al4V titanium sheets at high temperature, required to enhance the thermal dependency with a fourth-degree polynomial function of the homologous temperature instead of a linear one.

In [153], Novella et al. extended the Oyane-Sato criterion to high temperature and strain rate with application to AA6082 cross-wedge rolling. Observing that the critical Oyane-Sato damage value (D^*_{Oy}) depended on the test's temperature (T_{test}) and strain rate ($\dot{\varepsilon}_{\mathrm{test}}$), the authors suggested to incorporate these critical values in the criterion in the following way:

$$D = \int_0^{\bar{\varepsilon}_{\mathrm{f}}} \frac{1}{\mathrm{D}^*_{\mathrm{Oy}}(T_{\mathrm{test}}, \dot{\varepsilon}_{\mathrm{test}})} (1 + A\eta) d\bar{\varepsilon}_{\mathrm{p}} \tag{24}$$

This leads to a critical damage value equal to 1 in the given temperature and strain rate range.

The extension of coupled damage models can also be carried out to account for temperature and strain rate dependence. In [188], the Lemaitre damage potential modified in [25] was extended through a dependence to temperature and strain rate of each damage parameters. This extension required an extensive calibration approach due to the higher number of damage parameters. The final application to hot Nakajima tests for 22MnB5 steel sheets gave very convincing results. Based on Johnson's and Cook's former work, Bonora and Milella extended the Bonora coupled damage model by imposing a dependence of strain threshold, strain to fracture, and critical damage value to both strain rate and temperature [24].

Bambach and Imran [13] suggested an interesting extension of the GTN model dedicated to hot forming processes. Based on RVE simulations containing a rigid spherical inclusion, the authors generated numerical yield surfaces for elastic viscoplastic matrix material undergoing dynamic recrystallization (DRX). Based on these simulations, they proposed a modification of the GTN nucleation rate term which accounts for the yield stress, stress triaxiality ratio, Lode parameter, fracture toughness, and particles' size. This new void nucleation law enables to account for thermal softening mechanisms, but also for DRX-induced nucleation retardation for steels.

4.5. Calibration of failure criteria and damage models

Calibration of failure criteria and damage models is a cornerstone for an accurate prediction of ductile damage during material forming processes. It is essential that the experimental tests used for the calibration exhibit stress states and loading history conditions as close as possible to what the material experiences during the forming process. Then, depending on the approach selected, the identification methodology can differ.

Regarding uncoupled ductile failure criteria, the accuracy of the prediction depends on the accuracy of the measurement of the fracture strain. Experimental measurement of this fracture strain using DIC is challenging for sheet metal [123] and may be impossible for bulk metal forming. A hybrid experimental-numerical approach is generally considered [36]. Experiments with various stress states are carried out until fracture and the displacement to fracture is stored. Numerical simulations are then conducted and maximum numerical equivalent strains at experimental fracture stroke are considered as fracture strains. Such an approach requires a very accurate description of plasticity, in particular if one has to consider the high equivalent strain observed in necking areas. Differences of up to 30% in fracture strain depending on the mechanical preparation method of specimen were determined in [206]. Caution must also be taken regarding shear specimens for which failure usually occurs at free surfaces where stress triaxiality is usually significantly higher than 0. The plane torsion test is probably the only simple shear test that delivers a stress triaxiality of zero until fracture [205].

Thanks to its influence on the material behavior, the calibration of phenomenological continuum damage models (CDM) or coupled micromechanical damage models depends on direct or indirect quantification of damage. In their pioneering work, Lemaitre and Dufailly used CDM assumptions to propose a number of direct and indirect experimental techniques to measure the deformation-induced evolution of the damage parameter, D, that is required to calculate the effective stress [113]. Direct experimental techniques consider damage as a purely geometric characteristic that can be quantitatively measured employing density, void surface area fraction, or volume fraction measurements. For these types of measurements electron microscopy or X-ray tomography methods are typically employed. These methods are limited by inaccuracies introduced by specimen preparation and resolution issues, respectively [194]. Instead, indirect methods focus on the measurement of other material characteristics that are influenced by the presence of damage in the material. Lemaitre and Dufailly proposed two indirect, mechanical methods for the determination of the D parameter: probing of ductile damage through its effect on the elastic modulus or on hardness.

Apparent elastic modulus measurements can be carried out even during classical uniaxial tension tests [113]. Recently, this commonly employed approach is critically analysed [81]. These investigations revealed strong changes in apparent elastic modulus with increasing plastic strain in uniaxial tension tests that go beyond the effect of damage.

In forward rod extrusion the deviatoric stress state on the central axis is the same as in uniaxial tension tests. The hydrostatic stress state can be influenced by the process parameters [80]. High triaxiality η is reached for small strains and low triaxiality for high strains. Positive triaxiality values decrease the apparent Young's modulus significantly. High strains lead to negative triaxiality η and, thus, only to small reductions of the apparent Young's modulus compared to the initial material. Consequently, the correlation between strain and the decrease in apparent Young's modulus which is often proposed may also be connected to damage (Section 6, Fig. 38).

Modulus evolution can also be captured by micro-indentation experiments, employing the Oliver-Pharr approach [155]. This approach was also critically analysed for damage quantification on four different metallic materials. The significant levels of statistical variations observed [193] motivated the design of a modified approach that removes all microstructure effects other than damage itself from tested materials [195]. This method did successfully reveal the damage evolution relationship. However, the experimental complexity limits its widespread application to other metallic materials.

Hardness-based damage quantification assumes that the hardness is linearly proportional to the flow stress. Therefore, this methodology monitors the hardness degradation to assess the damage-induced changes in the flow stress [113]. Despite its popularity, a detailed analysis of this approach demonstrated that this method is not accurate, due to microstructure evolution accompanying damage evolution [193]. Similar to the indentation-modulus based measurements, when such microstructure effects are removed by heat treatments, damage effects can be captured [195]. Six such theoretically equivalent methodologies and the corresponding damage evolution curves are replotted in Fig. 19 to provide direct comparisons based on damage investigation on the same material [194].

These methodologies show two distinct regimes of damage evolution: an initial regime of slow damage accumulation followed by a regime of accelerated damage accumulation. Clear differences are also revealed [194]. From the statistical accuracy point of view, the area and volume fraction methodologies are clearly superior to the density methodology and especially to the three mechanical methodologies. The low precision of the mechanical methods attributed to the multitude of preparation steps can be improved to some extent by measurement repetition. Regarding systematic accuracy, however, the three mechanical methodologies agree within experimental uncertainty and provide more accurate damage parameters. This could be explained through the fundamental limitation of geometric methods to capture only geometric damage and not e.g. volumeless damage incidents such as closed micro-cracks.

In addition to such methodologies related to the quantification of damage, it is also common to identify damage parameters by inverse analysis on the whole load-stroke curves and based on the softening behavior due to damage accumulation [36]. However, inverse

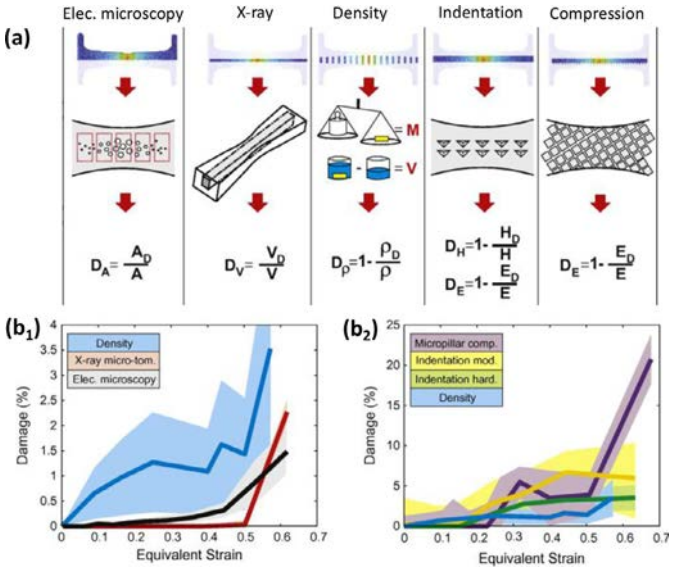

Fig. 19. Comparison of (a) the concepts and procedures, (b) the measured damage evolution, of six methodologies for damage quantification [194].

analysis based on load-stroke curves only may lead to non-unique parameter solutions as shown in [168], where inverse analysis was carried out using digital image correlation in addition to load-stroke curves to get a unique solution.

It is important to cover, as much as possible, the stress state range corresponding to the considered forming process. Brünig and coworkers also developed an interesting bi-axial test sample which enables a variation of loading conditions. They used this test successfully to calibrate their continuum damage model for various stress states [29].

Micromechanical models often require the use of microstructure observations. Contrary to SEM, X-ray tomography provides a non-destructive way of observing and quantifying nucleation, growth, and coalescence of voids [131]. Such observations enable the identification of GTN void-based parameters while other GTN parameters (q_1, q_2) may rely on unit-cell calculations. In [37], the authors combined both mechanical tests and in-situ X-ray microtomography observations to characterize the GTN parameters of a high carbon steel grade.

4.6. Which damage approach should I use?

The previous sections demonstrated that there is a large number of modeling approaches for damage and failure. Many models have been applied to predict the behavior in pretty simple tests such as notched tensile or Nakazima tests. However, it is essential to apply these models to real industrial forming applications for which loading paths are much more complex than conventional mechanical tests. The choice of the appropriate damage approach depends on the accuracy needed and on the effort one is willing to make for calibrating these models.

If you are interested in qualitative results and would like to know if new process conditions induce less damage than initial ones, then failure criteria may be sufficient. It remains important though to identify the failure dominating mechanism (high positive triaxiality, shear localization, plastic instability ...) to choose the most appropriate criterion. In this case there are only few parameters to identify. It must be noted though that such uncoupled failure criteria can also be used for predicting ductile fracture occurrence in a quantitative way (see Section 5). It requires a careful identification of damage parameters related to the process loading path and it also assumes that damage softening does not play a major role on fracture.

For more quantitative prediction of damage, the use of either phenomenological or micro-mechanical coupled damage models is recommended. These models account for damage softening and are more appropriate to handle complex and non-proportional loading paths. However, such models also come with drawbacks related to calibration complexity or mesh dependency. Such spurious numerical dependency requires the use of non-local approaches which must be calibrated carefully.

In both cases, the damage variable can serve as damage indicator and be used to address the mechanical strength of components during service.

Table 2 summarizes different model formulations in terms of their respective class (fracture criterion, micro-mechanically motivated coupled model, continuum damage model). The number of material parameters to be identified is usually directly related to the effort in

Table 2
Overview of modeling approaches with emphasis on effort for material parameter identification, "key contribution" to damage evolution "$f(\sigma)$" and exemplary applications. "√" indicates common practice, "(√)" rare application, "-" shows that this is usually not needed. The first three rows are basic and the fourth and fifth rows advanced failure criteria (Section 4.1), the sixth row micromechanical models (Section 4.3) the seventh and eighth rows phenomenological models (Section 4.2). For the failure criteria the number of parameters stand for those beyond $\bar{\varepsilon}_f$.

Model	# Parameters	Features		Parameter identification by			Comments	Exemplary applications		
		$f(\sigma)$	Comment	$F-u$	$\bar{\varepsilon}_f$	other		Bulk	Sheet	Hot
Cockcroft-Latham [47]	0	(σ_1)		√	√	stress state close to actual process	fast approaches, difficulties in shear	[143]	[74]	[99]
Oyane-Sato [156]	1-2	$\eta, (T, \dot{\varepsilon})$	(hot forming)					[4]	[172]	[153]
Rice-Tracey [163]	1	η						[66]	[74]	[170]
MMC [12]	6	$\eta, \bar{\theta}$		√	√	experiments with different stress states	robust, mesh-independent approach		[116] [144] [222]	
Lou et al. [125]	3	$\eta, \bar{\theta}$	cut-off for $\eta < 0$							
Gurson-Tvergaard-Needleman and extensions [68] [69]	8 - 10	$\eta, (\bar{\theta}, \tau_{\max})$; f (explicitly), nucleation [45], coalescence [208]	popular due to physical meaning and comparison to micrographs	(√)	-	unit cell calculations, identification by microstructure, large effort	decrease of strength; mesh-dependence; void closure possible; extensions for shear	[137]	[184]	[13]
Rousselier model and extension [166] [176]	7	η, f (explicitly)	Initial f_0 required	(√)	-	unit cell calculations, identification by microstructure, large effort	decrease of strength; mesh-dependence; void closure possible		[166] [176]	
Lemaitre [110]-Kachanov [96] model and extensions [25]	3-7	$\eta, (\tau_{\text{Max}})$; initiation threshold, damage value D	D affects physical properties: density ρ, Young's-modulus, ...	√	X	inverse identification, several stress states for extensions; large effort	decrease of strength and stiffness; mesh-dependence; extensions for $\eta < 0$ and shear; no voids closure	[171]	[197]	[84]

characterization experiments and calibration strategy. Here, only the parameters strictly governing damage or failure are listed. Characteristic features which usually represent the key contribution to the evolution of the fracture indicator, void volume fraction f, or actual damage value D are presented. The column "$F-u$" lists which models are usually identified by fitting parameters from force-displacement curves. Correspondingly, "$\overline{\varepsilon_f}$" indicates whether fracture strains are needed to identify the model parameters. In some cases, i.e. the Cockcroft-Latham criterion, the fracture strain directly represents the parameter. Finally, references where these models are typically applied to predict and analyse actual forming processes are listed.

5. Damage to failure: process limits

This section presents examples of prediction of failure occurrence in bulk and sheet metal forming processes, where the failure of the component is seen as the final evolution of damage. Indeed, this is the traditional way of applying damage analysis in metal forming. Failure criteria and damage models discussed in Section 4 are referred to in the section.

5.1. Porosity before forming

Cast parts, which can be characterized by cavities as a consequence of non-uniform solidification patterns or gases or both during the casting process, are often used as preforms in forging processes. These cavities are several orders of magnitudes larger than the voids discussed hitherto. However, the presence of such porosities may significantly affect the service life performances of the final products, therefore making their elimination during the first stages of forming-based process chains mandatory, otherwise they may evolve in cracks [108]. Their elimination is usually carried out through the conduction of hot forging or hot rolling processes just after casting, which must assure the mechanical closure of the cavities.

With the aim of studying the influence of the relevant process parameters on the evolution of cavities during forming, two approaches are available in the literature, namely explicit macroscopic and micro-analytical approaches [174]. The former is based on either physical or numerical simulations, which aim at establishing a correlation between the process parameters and cavities closure efficiency. In particular, it is proved that larger deformations and colder surface temperatures as well as shaped forging dies and high friction may be of help in increasing the voids closure efficiency. However, this approach is case-dependent. On the contrary, the micro-analytical approach is based on the description of a single cavity in an infinite matrix, but its starting assumptions are often far from real conditions.

To overcome the limitations of the above-mentioned approaches, a meso-scale one has recently emerged, based on the Representative Volume Element (RVE) method, which gives the chance to carry out simulations at the cavity-scale, making use of boundary conditions that are representative of macro-scale ones [173,55]. As example, explicit RVE simulations are used in [42] to calibrate a new cavity closure model taking into account the influence of both stress triaxiality and Lode parameter to overcome the hypothesis of axisymmetric loading.

The modeling of the voids in the RVE method is usually accomplished on the basis of statistical analyses. However, non-destructive X-ray Computed Tomography (CT), see also Section 3, may be applied for the 3D voids quantification before forging as well as in the validation phase of the RVE method [126].

The presence of shrinkage cavities in cast bars contributes to generate the so-called Mannesmann effect, namely a cavity formation along the bar longitudinal axis subjected to radial compression in metal forming. If, on one hand, this may affect the quality of the product obtained during cogging, cross-wedge rolling and rotary swaging of round bars, on the other hand, the Mannesmann effect is at the basis of the rotary piercing process to produce long and thick seamless tubes [62]. For proper modeling of the Mannesmann effect making use of damage laws, the initial voids fraction of the cast bar must be taken into account, as it strongly affects the tube steel behavior in terms of flow stress and ductility (Fig. 20).

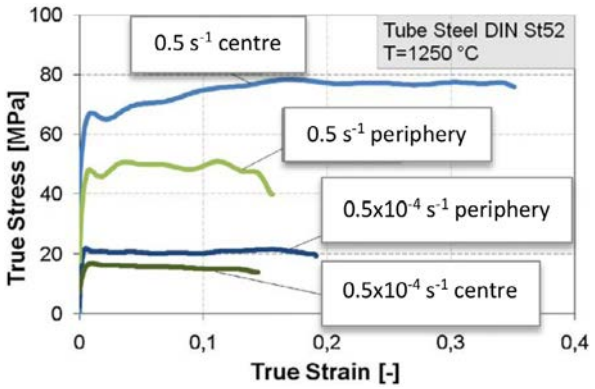

Fig. 20. Flow stress and ductility of samples extracted from different positions in a cast bar characterized by different voids fractions [62].

5.2. Bulk metal forming

In cold and hot bulk metal forming failures may appear as surface cracks and internal cracks. Surface cracks develop as a consequence of an unsuitable choice of the process parameters leading to tensile stress states. A comprehensive classification of fractures in forging together with their characteristics and crack growth directions can be found in [49], with particular reference to cold forging, but also extendable to hot forging.

Within cold forging, the different categories of failure criteria and damage models introduced in Section 4 are extensively applied to predict the fracture occurrence in single- and multi-step forging processes characterized by non-proportional and non-monotonic strain and stress paths.

One of the first attempts to use ductile failure criteria in single-step cold forging operations is presented in [66], showing acceptable prediction of fracture initiation sites, but emphasizing the need to select criteria with critical damage values that are constant at varying conditions of strains and stresses.

Different failure mechanisms, characteristic of different single-step cold forging operations, are predicted in [185] using a unique model, namely a Lemaitre variant damage model improved to account for quasi-unilateral damage evolution. This unique model is successfully applied to predict chevron cracking in forward extrusion of cylindrical billets and damage accumulation at the surface near the equator in upsetting of a tapered specimen, proving the model capability to be applied to single-step forming conditions characterized by different strain and stress paths.

The crack occurrence in multi-step cold-forged components, such as screw and shaft heads, can be satisfactorily predicted making use of both failure criteria and damage models. In [16], a linear damage accumulation law and the failure criterion based on the one by Bao and Wierzbicki, function of both the stress triaxiality and Lode parameter [216], are coupled providing a satisfactory agreement between the experimental and numerical fracture location as shown in Fig. 21.

The Lemaitre damage model is modified in [25] to take the crack closure effect and negative triaxiality limit into consideration. By considering hence the compressive damage evolution, similar fracture types in multi-step cold forging chains are predicted. In [25], the need to deal with material microstructures inducing anisotropic damage properties is also addressed. In particular, it is shown how damage anisotropy depending on orientation microstructure can be combined with grain flow orientation computation to predict ductile fracture.

Failure criteria as well as phenomenological and micromechanical damage models are applied in [34] to predict damage evolution and fracture occurrence in multi-step cold wire drawing and wire flat rolling, showing different predictive capabilities on the basis of the failure mechanisms. In case of multi-pass drawing of a pearlitic high carbon steel, all the applied criteria and models are able to predict the maximum damage location, but just the GTN micromechanical model can predict the instant of fracture, nevertheless it stressed the

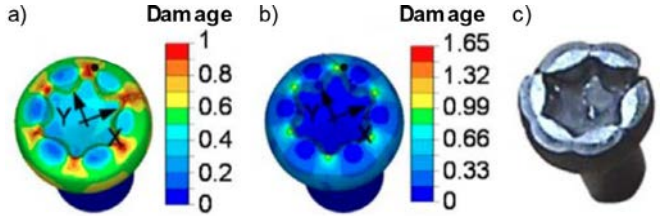

Fig. 21. (a) Simulated damage after multi-step cold forging according to the Oyane model, (b) and according to the failure criterion of Bao and Wierzbicki; (c) cracks in the industrially forged screw [16].

time-consuming procedure for its accurate calibration [37]. On the contrary, in case of one-pass wire flat rolling, only those failure criteria considering both the stress triaxiality and Lode parameter can correctly reproduce the damage localization.

In the context of cold forging, fracture is more likely to occur during those processes characterized by highly Severe Plastic Deformation (SPD), as is Equal Channel Angular Pressing (ECAP). The Lapovok et al. failure criterion (Section 4) is used in [106] to predict failure in grade 4 titanium subjected to Equal Channel Angular Pressing-Conform (ECAP-C) (Fig. 22), proving its capability to consider the effect of the high accumulated strain on the damage evolution. The same criterion was successfully applied to the prediction of fracture in a two-stage cold forming operation (wire-drawing followed by constrained upsetting) [105].

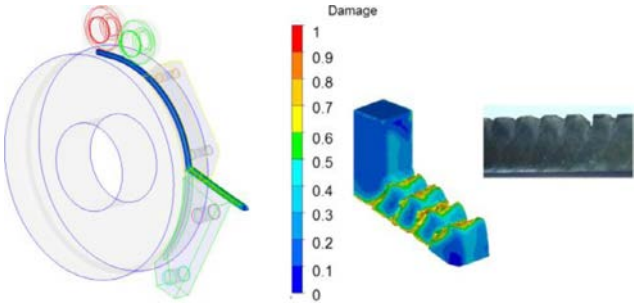

Fig. 22. (a) FEM model of the ECAP-C process; (b) experimental and numerically predicted periodic fractures [106].

The development of surface cracks in hot forging processes can be satisfactorily predicted by using fracture criteria with their critical damage variable accounting for the temperature and strain rate dependency. This approach is used in [8] in the case of the Cockcroft and Latham failure criterion to predict surface crack generation during the hot cogging process for producing a round bar from an ingot. The free surface cracks that may form on the surface undergoing free expansion are well predicted, showing that the minimization of the aspect ratio of the anvil edge geometry can minimize the surface crack generation. Also in [120], the effect of temperature and strain rate is incorporated into the critical damage variable of the normalized Cockcroft and Latham failure criterion to assess the fracture occurrence during a hot forging process, showing its capability to predict failure where the workpiece comes in contact with the die's corners (Fig. 23).

The development of internal cracks in hot-forged products, which may be the consequence of the evolution of pre-existing porosities, can be well described using both phenomenological and micromechanical damage models. The possible generation of damage in form of porosities during hot ring rolling is predicted in [210], using a

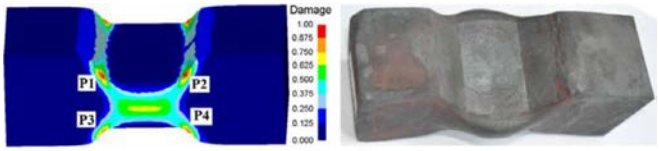

Fig. 23. Comparison between numerical and experimental fracture initiation sites in hot forging [120].

damage indicator based on the Oyane micromechanical model. The agreement between experimental and numerical damage fields is satisfactory, showing that a low ring growth rate can increase the susceptibility to damage when compared to high growth rate.

The same Oyane model modified to account for the influence of temperature and strain rate is coupled in [153] with the evolution of microstructural characteristics to predict the crack occurrence at the axis of bars deformed in hot cross wedge rolling processes. The cracks appearing at the centre of an AA6082-T6 aluminium alloy bar are replicated, proving a reduced formability at the highest testing temperatures as a consequence of hot shortness phenomena. The same typology of cracks during hot cross wedge rolling of high-speed railway axles is predicted in [85], making use of continuum damage mechanics coupled with microstructural evolution.

5.3. Sheet metal forming

In sheet forming processes, defects such as necking, tearing, and fracture may occur and adversely affect the quality of the formed product as a consequence of the attainment of a tensile state of stress higher than the one the material can sustain. Therefore, the process design and parameter choice must guarantee the achievement of the product's final shape without overcoming these limits. On the contrary, sheet cutting operations are designed to develop and propagate cracks, but with the aim of assuring a high-quality sheared surface.

As in the case of bulk forming, failure criteria, phenomenological, and micromechanical damage models have been extensively applied to describe damage evolution and fracture onset in sheet forming and cutting processes.

Shear fractures occurring in deep drawing can be satisfactorily predicted using failure criteria, as e.g. the MMC failure criterion. In [65] the model is calibrated on the basis of a hybrid experimental-numerical procedure which, in particular, makes use of cup drawing experiments providing insight into the out-of-plane shear fracture. The fracture location and onset instant in a deep-drawn triangular-shaped part made of AA6061-T4 aluminum alloy are predicted with good accuracy. The same failure criterion is employed in [116] to predict the initiation and propagation of cracks in deep drawing punch tests on TRIP 690 steel sheets. The simulated fracture location and magnitude of the punch travel are accurately reproduced for both circular and square punch geometries, showing the capability to predict shear-induced fractures.

Failure criteria taking into account the stress triaxiality can predict failure also in case of hole expansion and hole flanging processes. In [46], the hole expansion ratio and surface condition of TWIP and TRIP steel sheets are well predicted. In [95], failure when hole-flanging aluminium alloy sheets is predicted proving that, contrary to many sheet forming processes, the die radius has a weak effect on damaging the flange edge due to of its low negative stress triaxiality values.

The peculiar material behavior in sheet-bulk forming processes, as a consequence of the complex forming histories the material undergoes, requires the use of phenomenological damage models to correctly predict failure occurrence. In [87], tensile, elliptical bulge, circular bulge, and in-plane shear tests are used to calibrate the Lemaitre damage model to predict the evolution of voids during sheet-bulk forming of DC04 steel toothed components, pointing out the need for anisotropic evolution of damage.

Incremental sheet forming processes pose new challenges in predicting damage evolution and fracture occurrence as a consequence of the incremental nature of deformation, which calls for proper coupling of the conventional failure criteria and damage models with non-linear accumulation damage rules as well as accounting for the shear effect. The prediction capability of the MMC failure criterion is enhanced using a nonlinear damage accumulation rule in case of single-point incremental forming of AA6061-T6 aluminum alloy sheets [144]. The fracture criterion is calibrated on the basis of different tensile tests covering the process stress states and inverse analysis approaches for identifying the material coefficients, leading to a satisfactory prediction of the fracture depth (Fig. 24).

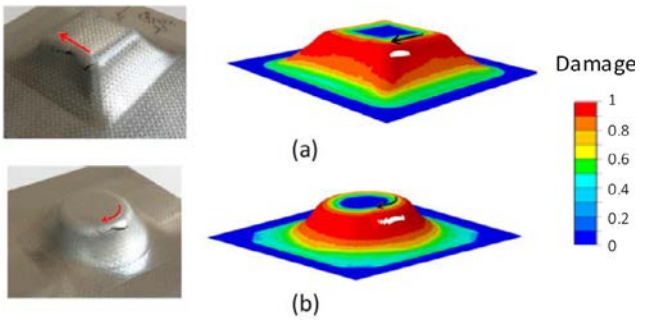

Fig. 24. Numerically predicted and experimental fracture locations in case of single point incremental forming of (a) truncated pyramid, and (b) truncated cone at varying wall angles [144].

Damage evolution and fracture occurrence are predicted in single-point incremental forming using the micro-mechanical GTN model modified to account for shear effect in [71]. It is shown that the modified GTN model predicts a premature material failure as a consequence of an inadequate coalescence criterion. On the contrary, the coupling of the GTN model with the physically based Thomason coalescence criterion helps in improving the prediction accuracy by delaying the onset of coalescence.

In [221], the Lemaitre damage model is adjusted to consider the nonlinear relationship between damage and plastic strain, proving its capability to predict fracture in the flange bottom area of the part during the splitting spinning process as a function of the roller feed ratio (Fig. 25).

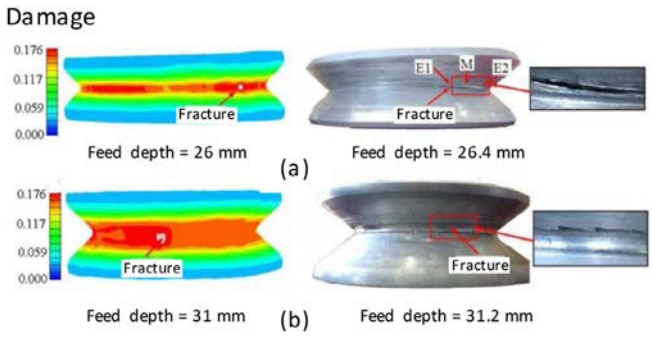

Fig. 25. Numerically predicted and experimental feed depths when fracture occurs during the splitting spinning process using roller feed ratios of (a) 3 mm/rev, and (b) 1 mm/rev [221].

A satisfactory prediction of fracture as a consequence of sheet cutting can be achieved when the effect of shear and compressive states of stress are considered. In [70], the Lemaitre damage model is modified taking into account the effect of shear and compression-dominated stress states on damage propagation, leading to reliable predictions of cutting forces and cutting surface appearance during shear cutting of dual phase steel sheets. A variant of the Lemaitre damage model to account for a compressive state of stress is also used to model the blanking process of high-carbon steel sheets in [88]. The comparison between experimental and numerically predicted cutting surfaces shows that the damage model with a crack-closure feature improves the prediction of the proportion between shear drop and burnished area (Fig. 26).

On the contrary, the failure criteria used in [75] to simulate mechanical trimming of hot stamped ultra-high-strength parts at room temperature give non satisfactory results, except for the MMC and Oyane criteria that predict the experimental results better. Nevertheless, a sensitivity analysis of the process parameters shows that the main crack initiates near the upper die and the cut surface profile can be improved by increasing the trimming die angle and blade radius, whereas the trimming clearance has a lower effect.

In the scope of sheet forming processes carried out at elevated temperature, the effect of temperature and strain rate on damage evolution and fracture onset is usually taken into account in the material coefficients of phenomenological damage models. In [188,84], the Lemaitre damage model is calibrated through a coupled experimental and numerical approach using tensile tests at varying temperature and strain rates to predict the fracture onset during hot stamping of boron steel sheets. In particular, in [84] the hot stamping process used to produce an automotive B-pillar is simulated with a satisfactory prediction of location of potential crack initiation, punch force, and thickness distribution.

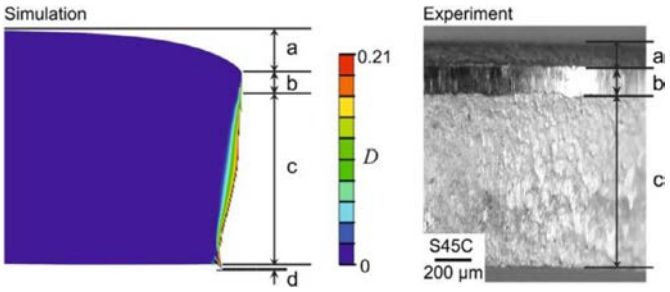

Fig. 26. Experimental and simulated cutting surfaces in blanking of high-carbon steel sheets [88].

6. Effects of forming-induced damage on product properties

Formed components are subject to various application-dependent requirements. The fulfilment of these requirements can be evaluated by the corresponding product properties. Product properties do not only depend on the choice of material, but also on the complete history of the material's processing, including forming operations.

During forming of metals, damage is initiated in their microstructure. Damage is not a failure per se, but it can lead to it during forming. Even before the fracture of parts damage affects the mechanical properties during service loadings. Nowadays, the focus in metal forming is on manufacturing products with known mechanical properties and not only on shaping materials, as described extensively in [199]. The forming process affects the basic product properties like hardness, residual stresses, and also the damage level.

The effect of strain hardening and residual stresses as product properties on the component performance is well known. In contrast, damage is only considered as the driving factor for fracture initiation during forming and not as a product property. For the investigation of the sole effect of damage on the product performance, a separation of the other effects strain hardening and residual stresses has to be done. This section explores the influence of process parameters in metal forming on the development of damage and the resulting product performance.

Influence of process-induced damage on final in-use properties is illustrated in [59], where half-blanking process parameters lead to different failure modes (Fig. 27a). Accounting for the simulation of the half-blanking stage leads to an improved load-displacement curve (red curve, Fig. 27b), both in terms of load-bearing capacity and ductile fracture prediction.

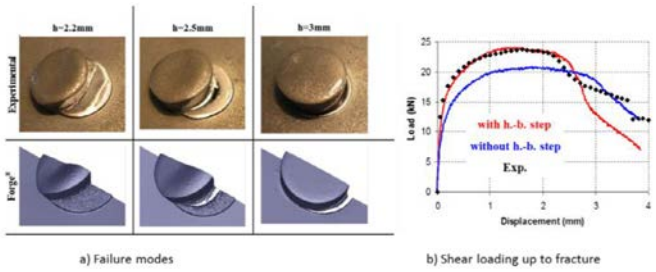

Fig. 27. a) Experimental and numerical shear failure modes for different half-blanking process parameters, b) shear load-displacement curves [59].

The sole effect of damage on the component properties such as fatigue strength has been experimentally proven for the first time in [198]. In cold forging and bending different damage levels were induced by various forming routes. The cold forging experiments

have been performed with the material 16MnCr5, whereas the air bending experiments with a dual phase steel.

For cold forging it was shown that damage influences the product properties even before chevron cracks occur in the core of the extrudate. Schwab investigated the effect of process parameters in forward rod extrusion on the fatigue behavior of the workpieces in his pioneering work [179]. At that time, he could not establish the relation to damage. In [198], the effect of distinct damage levels induced by forward rod extrusion on the fatigue strength was investigated. The damage level was modified by varying area reductions in extrusion. Finite element simulations showed that for a smaller strain the maximum axial tensile stress on the axis of the extrudate is higher than for larger strains (Fig. 28).

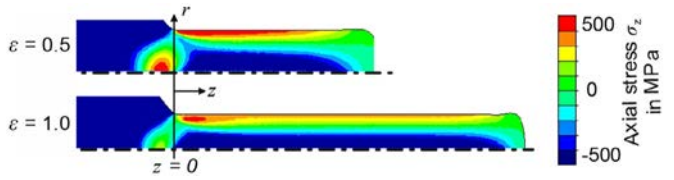

Fig. 28. Axial tensile stresses in the extrudate for various area reductions. Die cone angle $2\alpha = 90°$; Coulomb friction coefficient $\mu = 0.08$; elastic die (55NiCrMoV6); elastic-plastic workpiece (16MnCr5), [198].

The voids for the two extrusion setups were analysed with SEM. Fig. 29 shows two typical micrographs representative for a huge number of observed inclusions that the void nucleation is larger in samples with smaller strain and higher axial stress.

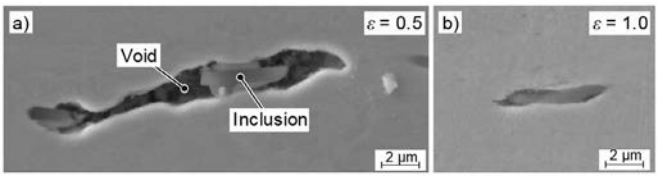

Fig. 29. Load path influence on damage evolution in 16MnCr5 extrudates for extrusion strains of a) $\varepsilon = 0.5$ and b) $\varepsilon = 1.0$, [198].

The effect of the damage on cyclic loading of the extrudates was analysed by multiple-step fatigue tests. It was shown that the samples taken from the core of the extrudate with lower extrusion strain fail significantly earlier than the samples with the higher extrusion strains (Fig. 30) due to different damage levels at the axis of the extrudate. It was shown that the effects of strain hardening and residual stresses can be excluded from the investigations of fatigue.

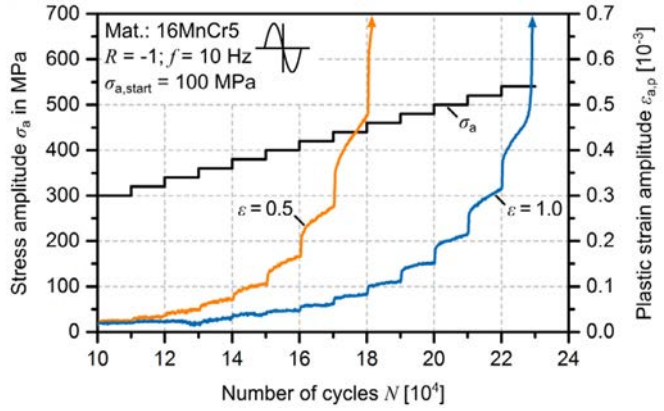

Fig. 30. Load path influence on damage evolution in 16MnCr5 extrudates for extrusion strains of a) $\varepsilon = 0.5$ and b) $\varepsilon = 1.0$, [198].

Also, the die cone angle has an influence on damage in forward rod extrusion. The load path, described by the triaxiality, is changed by different die cone angles. Measurements show that the void area fraction in forward rod-extruded parts is reduced by 74 % when

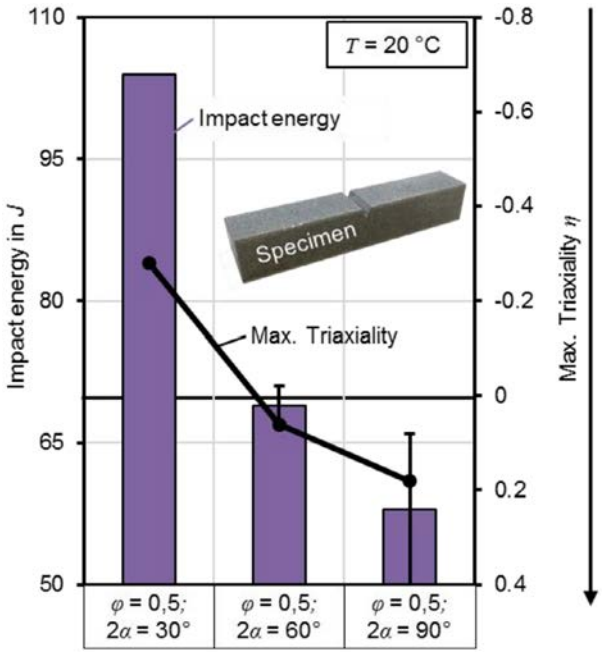

Fig. 31. Influence of triaxiality on the impact energy in forward rod extrusion for three die cone angles, but the same extrusion strain [78].

changing the die cone angles from 90° to 30° [79]. This leads to a 25% higher fatigue life, 79% higher impact energy (Fig. 31), and a 9% higher apparent Young's modulus. The influence of strain hardening and residual stresses on these results can be neglected [78].

For sheet metals the effect of superposed stresses on damage and, hence, on the product property fatigue strength are analysed in bending. Bending experiments without (Fig. 32a) and with elastomer cushion (Fig. 32b) were carried out.

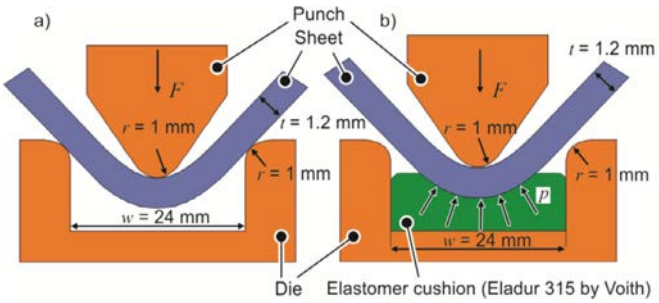

Fig. 32. a) Air bending and b) bending with an elastomer tool, [198].

An elastomer cushion is used to change the stress state and, hence, the triaxiality η by applying an additional counter pressure. A reduction of the triaxiality of 16 % is accomplished by using an elastomer tool ($\eta = 0.48$) compared to air bending ($\eta = 0.57$) at the tension side of the bending arc. SEM micrographs in Fig. 33 reveal that the number and area fraction of voids in air bending is higher than in bending with an elastomer tool.

Workpieces with identical geometry bent by air bending and bending with an elastomer cushion are evaluated in fatigue bending tests. The elastomer bent specimen shows a 20 % higher fatigue strength compared to the air bent specimen. This could be caused by strain hardening, damage, and residual stresses. Hardening and residual stress influences on the fatigue strength have been shown to be negligible. It was revealed that forming- induced damage is the reason for the higher fatigue strength, [198].

Although the fatigue life is improved by elastomer bending, the reproducibility is not fulfilled due to abrasion of the elastomer cushion. Also, the magnitude of the superposed pressure is much lower than the yield stress of the sheet. The stress state cannot be predicted accurately since the properties of the elastomer evolve during lifetime. Therefore, radial stress superposed bending (RSS-bending) was developed (Fig. 34),

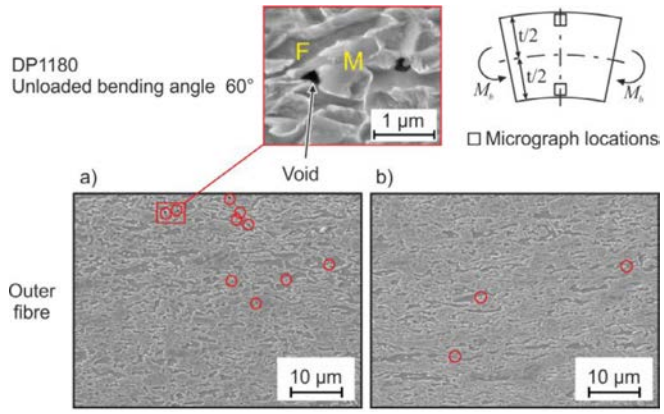

Fig. 33. SEM micrographs of the upper area (60μm x 40μm) in a sheet bent by a) air bending and b) with an elastomer tool. Red circles indicate the voids, [198]. F: Ferrite, M: Martensite

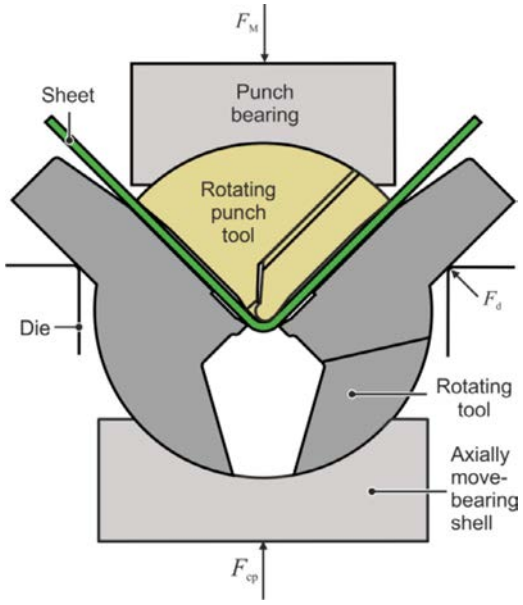

Fig. 34. Technical set-up of radial stress superposed bending [141].

[141]. Two tools rotate around the profile and superpose stresses on every point of the circumference. Due to the bending moment course the forming zone moves with this additional pressure. By adjusting the counter force $F_{cp,}$ the process is capable of applying predetermined compressive stresses and controlling the load path during bending, [142].

The superposition of stresses in RSS bending also leads to delayed damage evolution for a DP800 steel [141]. Additionally, this smaller amount of damage leads to a better product performance in impact tests (Fig. 35) and to a higher stiffness [138].

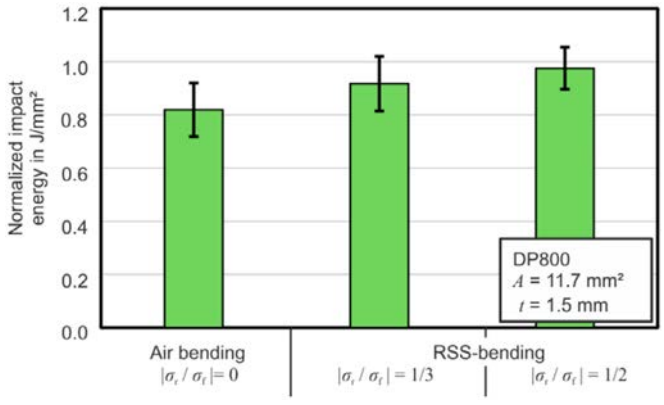

Fig. 35. Influence of radial stress superposition on the impact energy [140].

Besserer et al. investigated the fatigue behavior of parts produced by an orbital forming process [22]. In addition, the damage evolution was examined. They found out that both the forming process and cyclic loading cause an increase in ductile damage. They stated that in sheet-bulk metal forming the strain hardening has a positive effect on fatigue life and simultaneously damage has a negative effect. The effects of strain hardening and damage could not be separated.

In mechanical joining processes involving plastic strain and damage the importance of joining-induced damage to accurately predict the final joint strength was shown. Fayolle et al. [54] showed that the numerically predicted mechanical strength of self-pierced riveting joints is generally overestimated when compared to the corresponding experiment. The use of the Lemaitre damage model during the joining stage resulted in a damage field that was used as an input of mechanical strength simulations. Both the failure modes and joint's mechanical strength prediction were in good agreement with experiments [54]. Such a virtual chain of simulations coupling the joining stage and the analysis of its final mechanical strength set the stage for the optimization of forming parameters to improve the final mechanical strength properties. In [167], damage is considered as a product property in the clinching process and is used as an input parameter of the structural analysis stage. Optimizing two process parameters (punch radius R_p and lower tool depth P_m) led to an increase of the final strength of 13% in tension and 43% in shear. Fig. 36a/b shows the Lemaitre damage field after clinching for the initial configuration and the optimized ones. Fig. 36c) shows the final joint mechanical strength response surface for two clinching process parameters. The optimized solution (green cross) significantly improves the initial solution (red cross) with a higher fracture load.

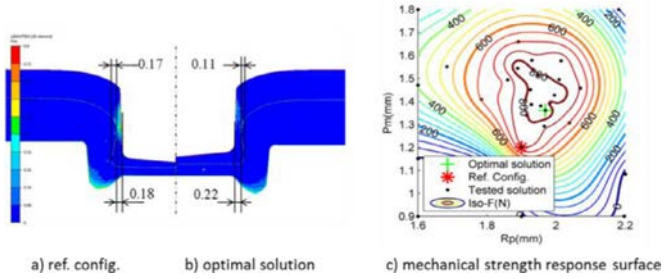

Fig. 36. Damage field at the end of the clinching process for the (a) reference, (b) optimized configurations and (c) response surface for the joint mechanical strength for two clinching process parameters, [54].

Kami et al. [97] showed that the anisotropic GTN damage model with Hill'48 quadratic yield criterion can be used to analytically construct the FLC of metallic sheets (Fig. 37). In general, the forming limit curve for the AA6016-T4 aluminium alloy predicted by the GTN

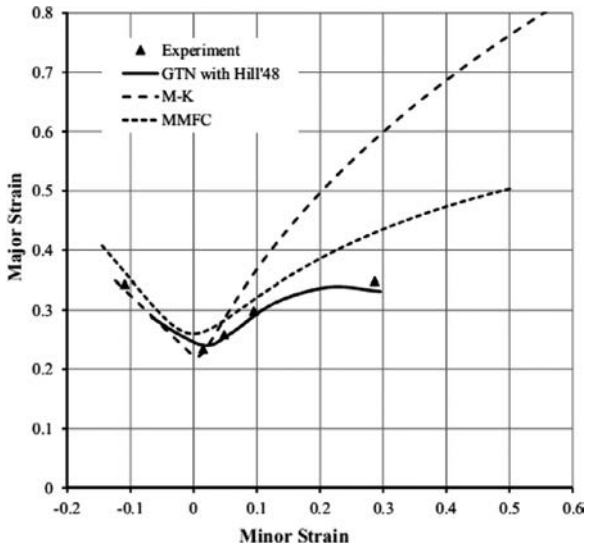

Fig. 37. Comparison of FLCs obtained by experimental and numerical investigations [97].

model were more accurate than those calculated with the Marciniak-Kuczynski (M−K) and modified maximum force criterion (MMFC) models without accounting for damage. This applies especially to the tension-tension part of the FLC.

For applications in which stiffness requirements need to be fulfilled the apparent Young's modulus is regarded as a product property. It is known that damage has an influence on the apparent Young's modulus since emerging voids lead to a decrease of the effective cross-section area normal to the load direction and, thus, to a decrease of the apparent Young's modulus. This decrease is illustrated by means of a simple tensile test with interim unloading in the classical work of Lemaitre and Dufailly [113]. The apparent Young's modulus is decreased in a tensile test of 99.99% copper from 98990 MPa at the beginning to 21700 MPa just before the rupture of the sample. This corresponds to a reduction of the apparent Young's modulus of 78%. Similarly, for a 16MnCrS5 steel Hering and Tekkaya [68] measured the change of apparent Young's modulus up to 0.2 plastic strains (Fig. 38a). In their results, a saturation of the apparent Young's modulus change is observed at plastic strain of about 0.1. However, both Lemaitre/Dufailly's and Hering/Tekkaya's results include the apparent Young's modulus change due to dislocation pile ups and not only due to damage. In order to isolate the effect of damage on the apparent Young's modulus, Hering and Tekkaya [68] conducted experiments at very high strains (beyond the saturation strains in Fig. 38a) and found that the apparent Young's modulus can even increase with plastic strain (Fig. 38b). This is explained through the fact that the specimens at very high strains are obtained by forward rod extrusion and that the triaxiality is increasing with increasing extrusion strain (Fig. 38b). The authors also give results for extruded specimens tested at the same extrusion strain, but with different stress triaxiality for different die cone angles and deliver, probably for the first time in literature, the sole effect of damage on the apparent Young's modulus.

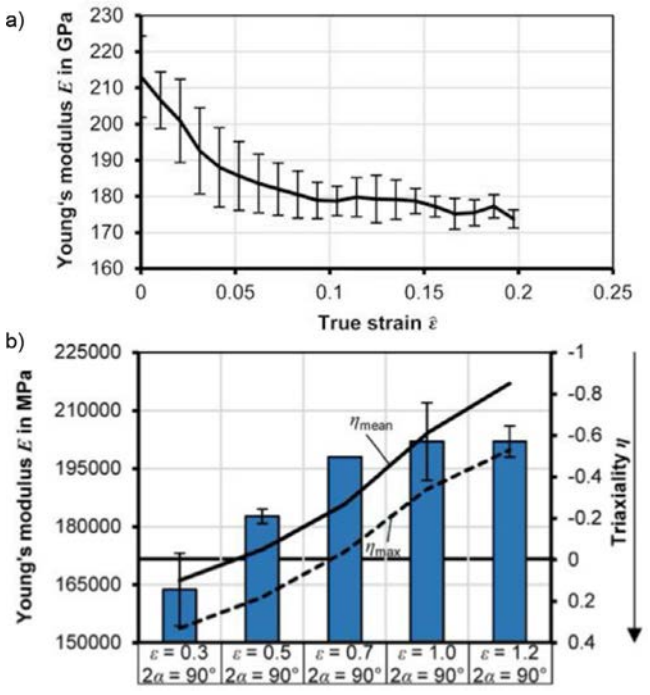

Fig. 38. Evolution of apparent Young's modulus during tensile test (16MnCrS5) a) Apparent Young's modulus change for small plastic strains in simple tension specimens with initially identical damage level, b) Apparent Young's modulus change for large plastic strains in extrusion specimens with different damage levels, [81].

In [157], the influence of the hole processing for two different steels (CP800 and DP780) on the equivalent failure strain in hole tension and expansion tests is investigated. The holes were produced by drilling and subsequent reaming or by hole punching (shearing). For both alloys the shearing reduces the edge formability (Fig. 39). The rate of damage accumulation is higher behind the sheared edge relative to the reamed edge due to the presence of pre-straining that promotes void evolution. The amount of pre-straining and damage introduced during shearing also

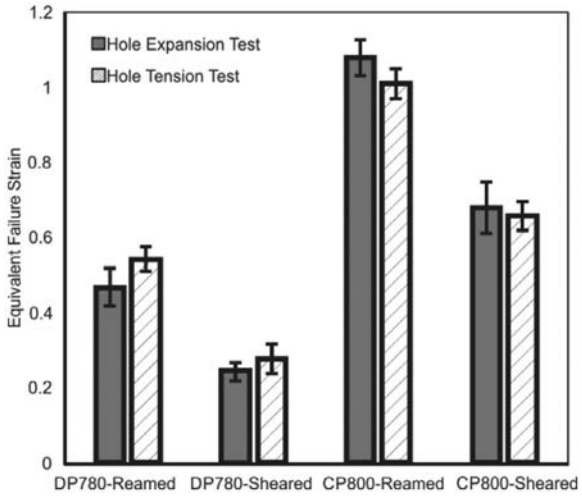

Fig. 39. Equivalent failure strain for two different steels and for two different hole processing methods investigated in hole expansion and tension tests [157].

depends on the microstructural constituents. CP800 provides better performance than DP780 steels due to the lower nucleation rate caused by the lower strength differential between the phases.

The hole expansion ratio of a punched sheet is compared to a punched sheet with an additional milling process to remove the damage accumulated by punching in [219]. The specimen prepared by the punching process consists of accumulated shearing damages and many micro-cracks. This damage promotes failure in the hole expansion test. If the hole edge region is processed by milling after the punching process, accumulated shearing damage is removed. Therefore, the hole expansion ratio is higher for the milled hole. Mohrbacher [147] reveals that initial damage can grow into macroscopic cracks upon stretching the cut edge. Laser cutting is recommended as a suitable method for avoiding damage initiation.

The effect of the hole punching process on the successive hole expansion for a DP 1000 steel sheet has been investigated in [72]. By numerical modeling the damage induced by punching and the irregularities of the fracture surface could be analyzed separately. The surface irregularities played a minor role for the edge crack sensitivity, while the damage due to manufacturing of the hole (e.g. blanking) had a significant effect. Fig. 40 reveals the experimental and numerical expansion ratios for two different hole processing technologies. The numerical results shown also include the surface irregularities. Simulations without the surface irregularities resulted in less than 5% higher hole expansion ratios.

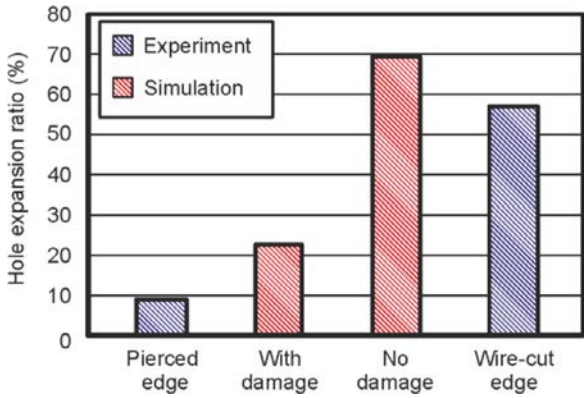

Fig. 40. Influence of damage on the hole expansion ratio for punched sheets made of DP 1000, [72].

In [58], the sheet-bulk process known as half-blanking carried out on high-strength low-carbon steel sheets is modelled through a newly developed phenomenological fracture criterion taking into account the complex multi-stage and non-proportional loading configurations that characterize the process. During this process very

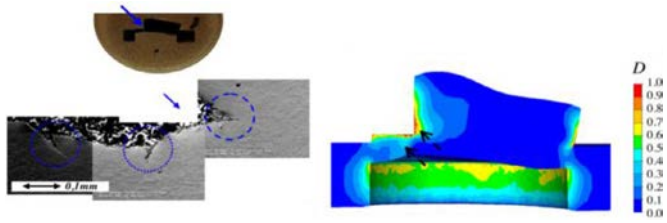

Fig. 41. Experimental and numerically predicted fracture location during shear tests following half blanking of high-strength low-carbon steel sheets [59].

high plastic strain can be reached because of stress triaxiality values below (-1/3). The influence of half-blanking process parameters on its final in-use properties during shearing (Fig. 41) shows the importance of accounting for damage created during the process stage.

The influence of the loading path on the damage evolution during hot calibre rolling has been investigated for the case-hardening steel 16MnCrS5 in [213]. To demonstrate the effect of stress path, compression, torsion and compression-torsion loadings have been investigated. Torsion loading generates more voids with larger void area fraction as compression or compression-torsion loading (Fig. 42).

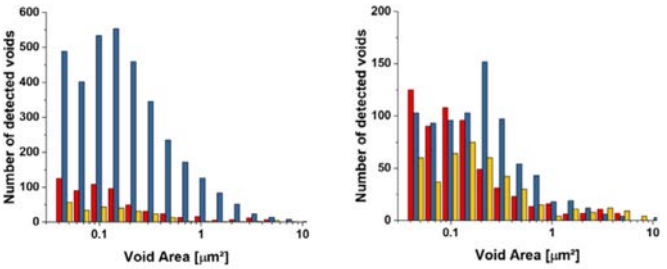

R12	Void Area Fraction		Void Number
As-recieved	$1.33_{x10^{-4}}$	$\pm 0.32_{x10^{-4}}$	582
R12-T	$8.52_{x10^{-4}}$	$\pm 0.54_{x10^{-4}}$	3496
R12-CT	$0.70_{x10^{-4}}$	$\pm 0.13_{x10^{-4}}$	258

R3	Void Area Fraction		Void Number
As-received	$1.33_{x10^{-4}}$	$\pm 0.32_{x10^{-4}}$	582
R3-T	$2.23_{x10^{-4}}$	$\pm 0.04_{x10^{-4}}$	804
R3-C	$1.95_{x10^{-4}}$	$\pm 0.07_{x10^{-4}}$	433

Fig. 42. Measurement of void area fractions under different load paths and different specimen geometries for 16MnCrS5 at 1100°C [213]. "T" stands for torsion loading and "C" for compression. R12 and R3 are the notch radii of the specimens.

7. Industrial utilization

In this section, the impact of damage as a process and product property is discussed. The section starts with the secured knowledge of the vigorous research field of ductile damage. The paradigm change based on this knowledge of damage is stated next. The benefits and the opportunities for industrial metal forming are compiled under the header industrial implications.

7.1. Secured Knowledge

The physics of damage at microstructural scale are largely understood. The mechanisms and the physical parameters influencing damage are well identified (Section 2). Regarding the mechanisms, it is known that ductile damage

- is a process driven by void nucleation, growth, and coalescence,
- is either promoted at high stress triaxiality values during plastic deformation, or,
- is promoted by plastic shear localization under nearly zero stress triaxiality,
- is a product property such as hardness, residual stresses etc.

For the implications in metal forming the most important secured knowledge is:

- The level of damage influences the performance of the product such as impact energy, fatigue life, stiffness, hole expansion ratios etc.
- The level of damage in a component can be controlled by designing the forming process properly. Reducing triaxiality results in a decreased void evolution in general.

In the modeling field the qualitative nature of damage can be described with various approaches from continuum-mechanics models to micro-scale physical models (Section 4). The effect of the forming process parameters on damage can be modelled qualitatively in a reliable way.

Finally, materials can be characterized by various established experiments as damage prone or resistant (Section 3). Also, the damage resistance designs of microstructures have been identified to allow the development of new materials.

7.2. Industrial implications

The recognition of ductile damage as a process of void evolution on microscopic scale and as a product property initiates a *paradigm change* in the metal forming industry. On the one hand, a transformation from phenomenological macroscopic plasticity to a microscopic view of plasticity is necessary and, on the other hand, the reorientation of the process design goals from formability to usability is initiated. These paradigm changes provide several benefits to the metal forming industry:

- Understanding the physics of the processes better. An impressive example for this is to recognize that large plastic strains do not necessarily induce more damage in the microstructure of the formed components. A relevant example given in Section 6 is cold rod extrusion. Large extrusion strains induce less damage than smaller extrusion strains (Fig. 43). Hence, it is not only the amount of plastic strain, but particularly also the stress state that influences the damage evolution in the component.

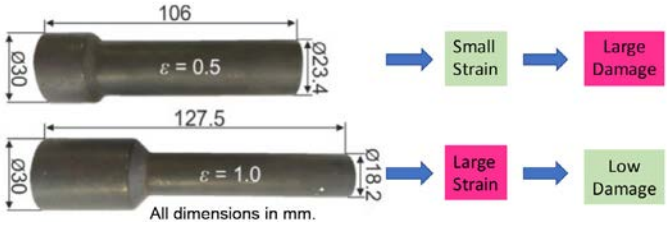

Fig. 43. Cold rod extrusion with small and large strains: it is not only the strain value that determines the damage level, it is also the stress triaxiality that matters, [198].

- The well described physics of ductile damage enable to revisit existing metal forming processes to deliver the same component from the same material with less damage and hence better product performance. Several examples for the process implementations have been shown in Section 6, but many more can be invented and applied under industrial circumstances. Sequences of forming processes are specially qualified for controlling the damage level. They provide many degrees of freedom to control damage, especially in combination with heat treatment. This will be explored further below.
- By the described experimental characterization methods, but also by the computational methods, the damage level in components can be determined and, hence, the performance of the component in service assessed more accurately than without considering the damage property. Consequently, safety factors for the components can be reduced and, thus, weight reductions achieved which contribute to lightweighting. Several promising feasible methodologies for assessing the damage level in components are already available such as density measurements, elastic modulus measurements, and impact energies. Fig. 44 shows the application of density measurements as a feasible methodology to assess the damage level of components with identical geometries [139] by distinct forming routes and hence distinct performances, [140]. This approach has a significantly larger accuracy than the density measurements described in [194] due to the much larger specimen volumes.
- Finally, considering failure by fracture or local instability as a final stage of damage evolution, the modern computational methods evolve towards a more precise determination of fracture or local

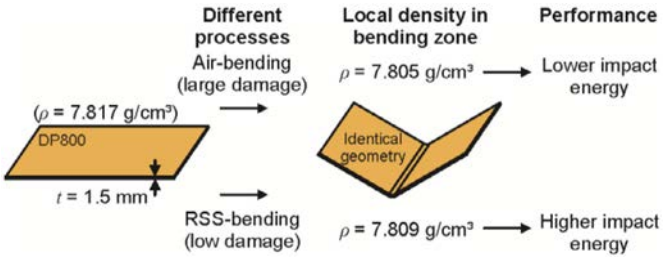

Fig. 44. Utilizing density measurement for formed parts to determine the damage level [139]: bending by two different processes leading to the same part geometry with different damage values and product performances (impact energy) [140].

necking incorporating loading paths in a concise manner not provided by the available methodologies such as forming limit curves (FLC) or simple fracture criteria. Using plasticity with coupled damage might be not necessary in general. Heibel et al. [77] showed that for dual phase steels plastic deformation leads to a small amount of void volume fraction and, hence, the influence on the effective stress is small. For such cases, uncoupled damage models or simple failure criteria are appropriate.

Various simple *process revisions* for lower damage and/or higher formability are possible today. Three basic physical principles are given in Table 3. These are revisions aiming for no change of the component geometry and no change of the basic composition of the component material. The corresponding possible process modifications are given for each physical principle and finally several known application examples are stated. It is important to note that these are just a few examples for possible modifications and applications. Considering the vast diversity of metal forming processes with more than 250 process variants, the immense opportunities of improving metal forming processes for products with reduced damage levels becomes obvious. This will move the goals of process design in metal forming from the traditional "formability" to the visionary "usability".

8. Outlook

Damage as an emerging concept in metal forming has been subject to extensive research over the last decades. Still, several unclear phenomena exist, requiring special focus in interdisciplinary research. These topics will be addressed in the next section. Also, the potential of considering damage in designing and forming components is not exhausted, bearing plenty more opportunities for the technological science-based developments. A vision about such future applications will conclude this section.

8.1. Open research questions

Despite the extensive knowledge accumulated, there are still several unresolved questions that need further extensive research. These topics can be divided into three groups:

i) Physics and quantification of damage: In most material models the damage variable is defined as the area or volume fraction of voids which is directly related to the damage-originated softening. In reality, however, the mechanical softening and the void area or volume fraction can be quite different. An example is given in Table 4 reflecting results for damage quantification after cold forging by three different methodologies [78]. Differences up to three orders of magnitude are recognized between the different damage increments for the same specimen. The correlation between mechanical softening and the void area or volume fraction needs to be further investigated in order to adapt the material models to depict both, the softening behavior as well as the void evolution, correctly. Further, damage leads to a complex, anisotropic change of the apparent elastic properties which are not considered in most of the material models.

ii) Modeling of damage: Components are generally produced by multiple forming operations. In the literature, however, it is common that only single forming stages are considered when it comes to the prediction of damage or fracture. In order to give a more realistic depiction of the void evolution, the whole process chain, including casting and rolling operations, needs to be considered. A first example for this approach is given by Schowtjak et al. [178] investigating the damage evolution in calibre rolling with subsequent cold forging. In the context of simulating the whole process chain, modeling the transition from continuum damage mechanics to discrete ductile fracture is a real challenge in the future to improve the prediction accuracy.

Plasticity models coupled with damage always result in mesh dependency in numerical modeling (Section 4.2). This mesh dependency can be alleviated in two ways: a) Characterizing damage model parameters for a specific element size and then ensuring that during the computations the element sizes remain below this limit. In this context the utilization of adaptive anisotropic mesh refinements is a promising approach [98] b) Using non-local formulations as applied to sheet bending in [186].

Table 3
Metal forming process modifications for lower damaged products based on modifying the stress state during plastic deformation.

Physical principle	Process modification	Application examples
Increasing hydrostatic pressure	Externally superposed pressure	Rod extrusion with counter pressure, bending against elastomer cushion
	Changing stress states through process parameter adaption	Modifying the cone angles in cold extrusion, bite modifications during rolling
Reducing straining over positive triaxiality values	Modifying process sequences	Adapting the straining per step in multi-stage extrusion, combining direct and reverse deep drawing
	Increase shear forming	Fine shear cutting, adiabatic cutting
Influencing strength of matrix material and/or inclusions	Using heat treatment processes	Various bulk and sheet metal forming processes with intermediate global or in-situ local heat treatments
	Modifying microstructural properties	Dual- or multi-phase materials with tailored matrix strengths

Table 4
Area fraction of damage D determined by various approaches after cold forging with $\varepsilon = 0.5$; $2\alpha = 90°$ of a 16MnCrS5, [78].

Parameter	Annealed undeformed material	After cold forging	Increase in damage ΔD
Density	7.825 g/cm^3	7.821 g/cm^3	$\Delta D = \left(\frac{1-\tilde{\rho}}{\rho}\right)^{\frac{2}{3}} = 6.40 \times 10^{-3}$
Void area fraction	6.60×10^{-5}	2.36×10^{-4}	$\Delta D = 1.70 \times 10^{-4}$
Apparent Young's modulus	211 GPa	182 GPa	$\Delta D = 1 - \frac{\tilde{E}}{E} = 1.37 \times 10^{-1}$

Scale-bridging models are very promising; however, the computational requirements of these models are far beyond acceptable limits for analysis of industrial scale processes.

Table 5 provides the effect of damage on the performance of a cold extruded 16MnCrS5 steel component [78]. Obviously, the larger die cone angle in extrusion generates higher damage in the component for the same plastic strain. It is striking to see that a void area fraction of the order 10^{-4} causes a change by 25% in fatigue tests and a change of 79% in Charpy impact tests. Currently, no reliable physical models are known being able to model this dependency of considerable performance change changes of the component after large strain forming by extremely small void fraction.

Table 5
Effect of damage on component performance after cold forward rod extrusion of 16MnCrS5, [78].

Properties	Cold forging $\varepsilon = 0.5$; $2\alpha = 90°$	Cold forging $\varepsilon = 0.5$; $2\alpha = 30°$	Difference
Void area fraction D	2.36×10^{-4}	5.90×10^{-5}	$\Delta D = 1.77 \times 10^{-4}$
Number of cycles to fracture N	163,000	205,000	ΔN = 42,000 (+ 25%)
Impact energy W in J	58	104	ΔW = 46 (+ 79%)

Finally, damage initiation, growth, and healing in warm and hot forming processes are not well understood. A promising attempt applied to metal forming processes is given by Bambach et al. [13] in which an extended GTN damage model coupling softening processes with void formation at inclusions is defined for hot forming.

iii) *Characterization of damage:* Damage models have several material-dependent parameters which must be determined experimentally (Section 4). Basically, these parameters are determined by inverse analysis. The most common approach for a parameter identification process is based on load-displacement data of notched tensile tests. Suárez et al. show that the void evolution predicted in the simulation do not fit well to the experimentally measured data obtained with CT investigations [187]. Load-displacement data does not have any information on the microstructure and, therefore, only characterize the damage-related softening and not the void evolution. In addition, since work hardening and damage-related softening have a contrary effect on the material's stiffness, the solution for the parameters is generally not unique. Only the use of full-field displacement measurement (DIC) as used in [168] can improve the solution. To this end, there are various solutions with different hardening behavior and damage evolution. Microstructural data have to be considered additionally in order to calibrate the model in terms of an accurate void evolution. Isik et al. identified a set of parameters for the void evolution of the GTN model for a DP600-graded steel based on an experimental void analysis [86]. Scientific articles that deal with the parameter identification of damage-related variables lack a validation in terms of microstructural data. While the macroscopic behavior of a forming process used for validation purposes is depicted well by the simulation, there is no explicit comparison of the predicted void evolution to the microstructure. Schowtjak et al. show that parameter identification for a GTN model based on force-displacement curves and/or DIC measurements supply good predictions for the plasticity, but are unable to predict the porosity after plastic deformations in bending [177]. This discrepancy does not only result from the assumption of spherical voids assumed in the classical GTN model. Using the measured porosity versus plastic strain values for the inverse parameter identification delivered not only good predictions for the plastic behavior, but also for the damage indicators by improving the porosity prediction by nearly two orders of magnitude.

8.2. Vision on damage

Future design of components is expected to include the imbedded damage as a product property as standard, allowing to decrease the safety factor of the design and, hence, the mass of the component. This will considerably contribute to lightweight designs and to resource efficiency. Re-visiting the process design in metal forming by considering the damage level of formed products as an objective of the process layout will be attributed higher, if not the highest priority in future. By this, metal forming will change from a "formability" objective to a "usability" objective. This will require an extended scale-bridging science-based manufacturing approach as described in this paper.

An exciting future development is the design of microstructures of metals to facilitate the control of damage to increase the performance of components. Needleman [151] envisions the controlled generation of voids during plastic deformation in order to delay or even stop crack propagation under the service loadings of the component. One impressive example for this vision is given by Glassmaker et al. [63] in which crack propagation is trapped through controlled cavities in glassy material and "ductile" deformation of such brittle materials is enabled. This idea could be also used for additively manufacturing (AM) pre-forms for forming complex components. The peculiar microstructural characteristics of AM alloys may lead to workability characteristics different from those of the wrought alloy of the same chemical composition. In [183], the hot workability of the Ti6Al4V titanium alloy produced by Selective Laser Melting (SLM) is investigated, showing favorable properties for hot working in terms of lower activation energy, lower peak stress, and faster globalization kinetics than the ones of the conventional wrought alloy with a lamellar microstructure. In the light of the above vision, the AM process can be designed to set a desirable distribution of voids. In subsequent steps, the superposed stresses, or a modified stress state lead to a retardation of damage evolution or directly to a reduction of damage.

Similarly, the phase design of advanced steels can be used to achieve a microstructure with special damage resisting properties. The development of design guidelines for the production of dual-phase damage-resistant steels is investigated by [76]. The investigations show that the homogeneous complex phase steels are more damage-tolerant.

The use of finite element simulation at micro and meso scale will help getting a better understanding of damage mechanisms under various loading paths [182]. In particular, accounting for the heterogeneity of the microstructure is the key to nucleation mechanisms. In-situ X-ray tomo- and laminography tests represent non-destructive promising techniques to follow void history from nucleation to growth and coalescence under various stress states and possibly non-proportional loading paths. Combined with Digital Volume Correlation (DVC) and FE-modeling at the microscale [181] it is possible to model damage mechanisms with the exact microstructure and exact boundary conditions. Such an attempt was done in [32] on nodular graphite cast iron where the local strain in the ligament prior to coalescence was estimated by DVC in [31] and by FE computation in [207], Fig. 45.

The analysis of the loading path on nucleation and growth mechanism is also made possible thanks to this multi-scale approach [169],

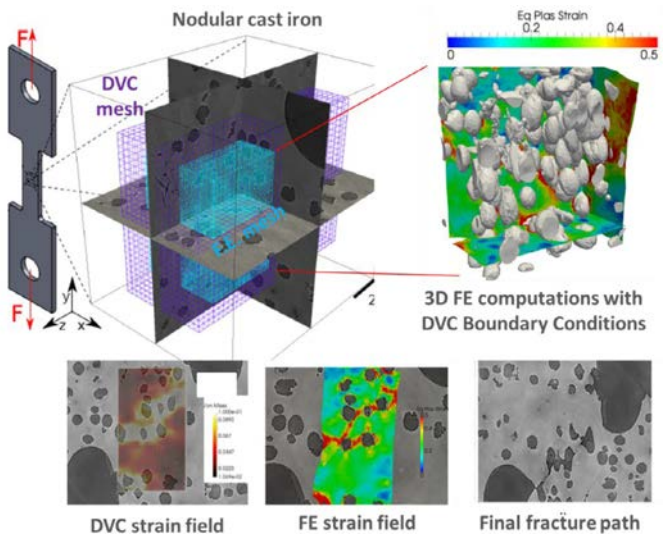

Fig. 45. Finite element computations on real microstructures obtained from SRCL (Synchrotron Radiation Computed Laminography) observations and with boundary conditions measured by DVC. Comparisons with experimental observations of nodular graphite cast iron, [207].

which could be useful regarding process stage optimization strategies. The extension of such techniques for other alloys, including multiphase materials, is promising for the understanding of damage mechanisms, for the optimization of forming process strategies, and for the engineering and design of new alloys.

Characterizing damage for practical industrial usage is clearly an emerging research field. The challenges are to efficiently perform large-scale measurements of micro-structural entities and develop methodologies to quickly assess macroscopic metal formed components. Hoefnagels et al. [82] used a semi-automatic statistical identification algorithm that identifies all damage incident areas in a statistically relevant area. It also reveals the damage mechanism (Fig. 46).

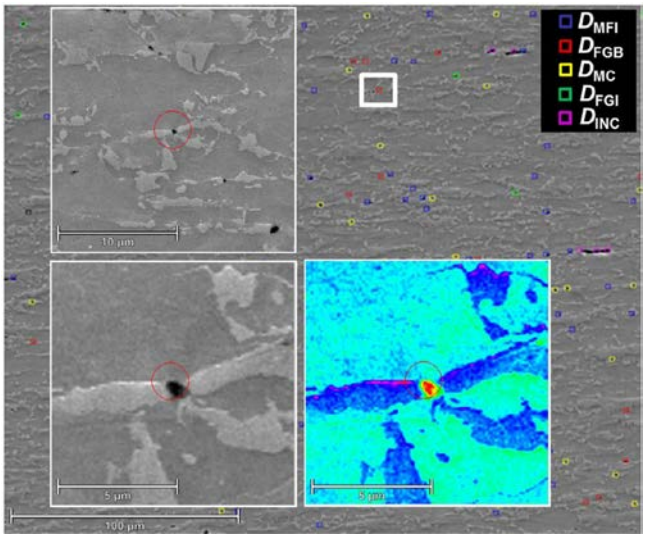

Fig. 46. Screen capture of semi-automatic statistical damage identification algorithm at different resolutions (Martensite cracking (MC), Ferrite Interface damage (MFI), damage at a ferrite grain boundary (FGB), damage at the ferrite grain interior (FGI), damage around inclusions (INC)). [82]

Kusche et al. used an artificial intelligence approach to identify the occurring damage mechanism [103]. The global and high-resolution methodology for damage quantification was used for products bent with air and RSS bending [139]. The higher damage evolution in air-bent products was also revealed by locally destructive density measurements. Another method for obtaining more information about the damage mechanisms in metal forming is gained by the combination of EDX and SEM analysis. Hering et al. revealed that the damage mechanisms can be identified and information about each damage site can be gathered [79]. The influence of a higher hydrostatic pressure was also shown with density measurements.

Finally, understanding ductility for incremental forming processes, where repeated deformation enables extremely high strains without fracture will, be a future research field. Calibration of failure criteria or damage models by conventional mechanical tests is not appropriate for such processes.

Acknowledgment

The authors wish to thank all CIRP STC-F members and the CIRP Editorial Committee for their valuable contributions during the discussion and review of the paper. The excellent contributions of Prof. S. Münstermann (RWTH Aachen University) and Prof. J. Lian (Aalto University), especially for Section 2 “Mechanisms of ductile damage”, are highly appreciated. The extensive support of Dr. T. Clausmeyer, Dr. O. Hering, Dr. R. Meya, and Mr. A. Schowtjak (TU Dortmund University, Germany) in the preparation of the paper is highly acknowledged and appreciated. We would also like to thank Mrs. J. Brandt for the language editing of the article. Parts of the paper have been supported by the German Research Foundation within the Collaborative Research Centre TRR188 “Damage Controlled Forming Processes” (Sub-Project #A02, A05, S01) – project number 278868966.

References

[1] Achouri M, Germain G, dal Santo P, Saidane D (2013) Experimental Characterization And Numerical Modeling Of Micromechanical Damage Under Different Stress States. *Materials & Design* 50:207–222.
[2] Achouri M, Germain G, dal Santo P, Boude S, Lebrun J, Lou, Saidane D (2011) Development Of A Microscopic Damage Model For Low Stress Triaxiality. *Key Engineering Materials* 473:460–467.
[3] Ahmad E, Manzoor T, Ali KL, Akhter JI (2000) Effect Of Microvoid Formation On The Tensile Properties Of Dual-Phase Steel. *Journal of Materials Engineering and Performance* 9/3:306–310.
[4] Alberti N, Barcellona A, Masnata A, Micari F (1993) Central Bursting Defects In Drawing And Extrusion: Numerical And Ultrasonic Evaluation. *CIRP Annals* 42/1:269–272.
[5] Andrade FXC, Feucht M, Haufe A, Neukamm F (2016) An Incremental Stress State Dependent Damage Model For Ductile Failure Prediction. *International Journal of Fracture* 200/1–2:127–150.
[6] Andrade Pires FM, César de Sá JMA, Costa Sousa L, Natal Jorge RM (2003) Numerical Modelling Of Ductile Plastic Damage In Bulk Metal Forming. *International Journal of Mechanical Sciences* 45/2:273–294.
[7] Argon AS, Im J, Safoglu R (1975) Cavity Formation From Inclusions In Ductile Fracture. *Metallurgical Transactions A* 6/4:825–837.
[8] Arikawa T, Yamabe D, Kakimoto H (2014) Influence Of Anvil Shape Of Surface Crack Generation In Large Hot Forging Process. *Procedia Engineering* 81:480–485.
[9] ASM International. Handbook. *ASM Handbook: Volume 12: Fractography*, Metals handbook.
[10] Babout L, Brechet Y, Maire E, Fougères R (2004) On The Competition Between Particle Fracture And Particle Decohesion In Metal Matrix Composites. *Acta Materialia* 52/15:4517–4525.
[11] Babout L, Maire E, Fougères R (2004) Damage Initiation In Model Metallic Materials: X-Ray Tomography And Modelling. *Acta Materialia* 52/8:2475–2487.
[12] Bai Y, Wierzbicki T (2008) A New Model Of Metal Plasticity And Fracture With Pressure And Lode Dependence. *International Journal of Plasticity* 24/6:1071–1096.
[13] Bambach M, Imran M (2019) Extended Gurson–Tvergaard–Needleman Model For Damage Modeling And Control In Hot Forming. *CIRP Annals* 68/1:249–252.
[14] Bao Y, Wierzbicki T (2004) On Fracture Locus In The Equivalent Strain And Stress Triaxiality Space. *International Journal of Mechanical Sciences* 46/1:81–98.
[15] Bao Y, Wierzbicki T (2005) On The Cut-Off Value Of Negative Triaxiality For Fracture. *Engineering Fracture Mechanics* 72/7:1049–1069.
[16] Bariani PF, Bruschi S, Ghiotti A, Simionato M (2011) Ductile Fracture Prediction In Cold Forging Process Chains. *CIRP Annals* 60/1:287–290.
[17] Barnby JT, Shi YW, Nadkarni AS (1984) On The Void Growth In C-Mn Structural Steel During Plastic Deformation. *International Journal of Fracture* 25/4:273–283.
[18] Bažant ZP, Jirásek M (2002) Nonlocal Integral Formulations Of Plasticity And Damage: Survey Of Progress. *Journal of Engineering Mechanics* 128/11:1119–1149.
[19] Benzerga AA, Leblond J-B (2010) Ductile Fracture By Void Growth To Coalescence. *Advances in Applied Mechanics* 44:169–305.
[20] Benzerga AA, Surovik D, Keralavarma SM (2012) On The Path-Dependence Of The Fracture Locus In Ductile Materials – Analysis. *International Journal of Plasticity* 37:157–170.
[21] Benzerga AA, Besson J, Batisse R, Pineau A (2002) Synergistic Effects Of Plastic Anisotropy And Void Coalescence On Fracture Mode In Plane Strain. *Modelling and Simulation in Materials Science and Engineering* 10/1:73–102.
[22] Besserer H-B, Hildenbrand P, Gerstein G, Rodman D, Nürnberger F, Merklein M, Maier HJ (2016) Ductile Damage And Fatigue Behavior Of Semi-Finished Tailored Blanks For Sheet-Bulk Metal Forming Processes. *Journal of Materials Engineering and Performance* 25/3:1136–1142.
[23] Besson J (2010) Continuum Models Of Ductile Fracture: A Review. *International Journal of Damage Mechanics* 19/1:3–52.
[24] Bonora N, Milella PP (2001) Constitutive Modeling For Ductile Metals Behavior Incorporating Strain Rate, Temperature And Damage Mechanics. *International Journal of Impact Engineering* 26/1–10:53–64.
[25] Bouchard P-O, Bourgeon L, Fayolle S, Mocellin K (2011) An Enhanced Lemaitre Model Formulation For Materials Processing Damage Computation. *International Journal of Material Forming* 4/3:299–315.
[26] Bridgman PW (1945) Effects Of High Hydrostatic Pressure On The Plastic Properties Of Metals. *Reviews of Modern Physics* 17/1:2–4.
[27] Brozzo P, Deluca B, Rendina R (1972) A New Method For The Prediction Of Formability Limits In Metal Sheets. In: In: *Proceedings of the 7th Biennal Conference of IDDRG, Amsterdam*.
[28] Brünig M (2003) An Anisotropic Ductile Damage Model Based On Irreversible Thermodynamics. *International Journal of Plasticity* 19/10:1679–1713.
[29] Brünig M, Brenner D, Gerke S (2015) Stress State Dependence Of Ductile Damage And Fracture Behavior: Experiments And Numerical Simulations. *Engineering Fracture Mechanics* 141:152–169.
[30] Brünig M, Gerke S (2011) Simulation Of Damage Evolution In Ductile Metals Undergoing Dynamic Loading Conditions. *International Journal of Plasticity* 27/10:1598–1617.
[31] Buljac A, Helfen L, Hild F, Morgeneyer TF (2018) Effect Of Void Arrangement On Ductile Damage Mechanisms In Nodular Graphite Cast Iron: In Situ 3d Measurements. *Engineering Fracture Mechanics* 192:242–261.
[32] Buljac A, Shakoor M, Neggers J, Bernacki M, Bouchard P-O, Helfen L, Morgeneyer TF, Hild F (2017) Numerical Validation Framework For Micromechanical Simulations Based On Synchrotron 3d Imaging. *Computational Mechanics* 59/3:419–441.
[33] Calcagnotto M, Adachi Y, Ponge D, Raabe D (2011) Deformation And Fracture Mechanisms In Fine- And Ultrafine-Grained Ferrite/Martensite Dual-Phase Steels And The Effect Of Aging. *Acta Materialia* 59/2:658–670.
[34] Cao T-S, Bobadilla C, Montmitonnet P, Bouchard P-O (2015) A Comparative Study Of Three Ductile Damage Approaches For Fracture Prediction In Cold Forming Processes. *Journal of Materials Processing Technology* 216:385–404.

[35] Cao T-S, Gachet J-M, Montmitonnet P, Bouchard P-O (2014) A Lode-Dependent Enhanced Lemaitre Model For Ductile Fracture Prediction At Low Stress Triaxiality. *Engineering Fracture Mechanics* 124–125:80–96.

[36] Cao T-S, Gaillac A, Montmitonnet P, Bouchard P-O (2013) Identification Methodology And Comparison Of Phenomenological Ductile Damage Models Via Hybrid Numerical–Experimental Analysis Of Fracture Experiments Conducted On A Zirconium Alloy. *International Journal of Solids and Structures* 50/24:3984–3999.

[37] Cao TS, Maire E, Verdu C, Bobadilla C, Lasne P, Montmitonnet P, Bouchard PO (2014) Characterization Of Ductile Damage For A High Carbon Steel Using 3D X-Ray Micro-Tomography And Mechanical Tests - Application To The Identification Of A Shear Modified Gtn Model. *Computational Materials Science* 84:175–187.

[38] Cao TS (2017) Models For Ductile Damage And Fracture Prediction In Cold Bulk Metal Forming Processes: A Review. *International Journal of Material Forming* 10/2:139–171.

[39] César de Sá JMA, Areias PMA, Zheng C (2006) Damage Modelling In Metal Forming Problems Using An Implicit Non-Local Gradient Model. *Computer Methods in Applied Mechanics and Engineering* 195/48–49:6646–6660.

[40] Chaboche JL (1984) Anisotropic Creep Damage In The Framework Of Continuum Damage Mechanics. *Nuclear Engineering and Design* 79/3:309–319.

[41] Chae D, Koss DA (2004) Damage Accumulation And Failure Of Hsla-100 Steel. *Materials Science and Engineering: A* 366/2:299–309.

[42] Chbihi A, Bouchard P-O, Bernacki M, Pino Muñoz D (2017) Influence Of Lode Angle On Modelling Of Void Closure In Hot Metal Forming Processes. *Finite Elements in Analysis and Design* 126:13–25.

[43] Chow CL, Wang J (1987) An Anisotropic Theory Of Continuum Damage Mechanics For Ductile Fracture. *Engineering Fracture Mechanics* 27/5:547–558.

[44] Chow CL, Wei Y (1991) A Model Of Continuum Damage Mechanics For Fatigue Failure. *International Journal of Fracture* 50/4:301–316.

[45] Chu CC, Needleman A (1980) Void Nucleation Effects In Biaxially Stretched Sheets. *Journal of Engineering Materials and Technology* 102/3:249.

[46] Chung K, Ma N, Park T, Kim D, Yoo D, Kim C (2011) A Modified Damage Model For Advanced High Strength Steel Sheets. *International Journal of Plasticity* 27/10:1485–1511.

[47] Cockcroft MG, Latham DJ (1968) Ductility And Workability Of Metals. *Journal of the Institute of Metals* 99:33–39.

[48] Cox TB, Low JR (1974) An Investigation Of The Plastic Fracture Of AISI 4340 And 18 Nickel-200 Grade Maraging Steels. *Metallurgical Transactions* 5/6:1457–1470.

[49] Dodd B, Ollilainen V, Limin L (1993) *Final Report By The Materials And Defects Sub-Group Of The ICFG on LHC Classification Of Defects, Final Report By The Materials And Defects Sub-Group Of The ICFG on LHC Classification Of Defects*, Japan, Osaka.

[50] Dunand M, Mohr D (2017) Predicting The Rate-Dependent Loading Paths To Fracture In Advanced High Strength Steels Using An Extended Mechanical Threshold Model. *International Journal of Impact Engineering* 108:272–285.

[51] Edelson BI, Baldwin WMJ (1962) The Effect Of Second Phases On The Mechanical Properties Of Alloys. *Transactions of the American Society for Metals* 55:230–250.

[52] Edmonds DV, He K, Rizzo FC, De Cooman BC, Matlock DK, Speer JG (2006) Quenching And Partitioning Martensite—A Novel Steel Heat Treatment. *Materials Science and Engineering A* 438440:25–34.

[53] Erdogan M (2002) The Effect Of New Ferrite Content On The Tensile Fracture Behaviour Of Dual Phase Steels. *Journal of Materials Science* 37/17:3623–3630.

[54] Fayolle S, Bouchard P-O, Mocellin K (2014) Modelling The Strength Of Self-Piercing Riveted Joints. *Self-Piercing Riveting*, Elsevier, 79–107.

[55] Feng C, Cui Z, Liu M, Shang X, Sui D, Liu J (2016) Investigation On The Void Closure Efficiency In Cogging Processes Of The Large Ingot By Using A 3-D Void Evolution Model. *Journal of Materials Processing Technology* 237:371–385.

[56] Freudenthal AM, Geiringer H (1958) The Mathematical Theories Of The Inelastic Continuum. in Flügge S, (Ed.) *Elasticity and Plasticit (Elastizität und Plastizität)*, Springer Berlin Heidelberg, Berlin, Heidelberg, 229–433.

[57] Fu R, Feng D, Chen X (2007) Effects Of Undersized Inclusions On Ductile Fracture Behavior Of Feni42 Alloy In Sheet Tension. *Journal of Iron and Steel Research, International* 14/5:53–58.

[58] Gachet J-M, Delattre G, Bouchard P-O (2014) Fracture Mechanisms Under Monotonic And Non-Monotonic Low Lode Angle Loading. *Engineering Fracture Mechanics* 124–125:121–141.

[59] Gachet J-M, Delattre G, Bouchard P-O (2015) Improved Fracture Criterion To Chain Forming Stage And In Use Mechanical Strength Computations Of Metallic Parts – Application To Half-Blanked Components. *Journal of Materials Processing Technology* 216:260–277.

[60] Garrison WM, Moody NR (1987) Ductile Fracture. *Journal of Physics and Chemistry of Solids* 48/11:1035–1074.

[61] de Geus TWJ, Peerlings RHJ, Geers MGD (2015) Microstructural Topology Effects On The Onset Of Ductile Failure In Multi-Phase Materials – A Systematic Computational Approach. *International Journal of Solids and Structures* 67–68:326–339.

[62] Ghiotti A, Fanini S, Bruschi S, Bariani PF (2009) Modelling Of The Mannesmann Effect. *CIRP Annals* 58/1:255–258.

[63] Glassmaker NJ, Jagota A, Hui C-Y, Noderer WL, Chaudhury MK (2007) Biologically Inspired Crack Trapping For Enhanced Adhesion. *Proceedings of the National Academy of Sciences* 104/26:10786–10791.

[64] Gologanu M, Leblond J-B, Perrin G, Devaux J (1997) Recent Extensions Of Gurson's Model For Porous Ductile Metals. in Suquet P, (Ed.) *Continuum Micromechanics*, Springer Vienna, Vienna, 61–130.

[65] Gorji MB, Mohr D (2018) Predicting Shear Fracture Of Aluminum 6016-T4 During Deep Drawing: Combining Yld-2000 Plasticity With Hosford–Coulomb Fracture Model. *International Journal of Mechanical Sciences* 137:105–120.

[66] Gouveia BPPA, Rodrigues JMC, Martins PAF (1996) Fracture Predicting In Bulk Metal Forming. *International Journal of Mechanical Sciences* 38/4:361–372.

[67] Gross AJ, Ravi-Chandar K (2017) On The Deformation And Failure Of Al 6061-T6 In Plane Strain Tension Evaluated Through In Situ Microscopy. *International Journal of Fracture* 208/1–2:27–52.

[68] Gurson AL (1977) Continuum Theory Of Ductile Rupture By Void Nucleation and Growth: Part I—Yield Criteria And Flow Rules For Porous Ductile Media. *Journal of Engineering Materials and Technology* 99/1:2–15.

[69] Gurson AL (1975) Plastic Flow And Fracture Behavior Of Ductile Materials Incorporating Void Nucleation. *Growth and Interaction*, Brown University.

[70] Gutknecht F, Steinbach F, Hammer T, Clausmeyer T, Volk W, Tekkaya AE (2016) Analysis Of Shear Cutting Of Dual Phase Steel By Application Of An Advanced Damage Model. *Procedia Structural Integrity* 2:1700–1707.

[71] Guzmán CF, Yuan S, Duchêne L, Saavedra Flores EI, Habraken AM (2018) Damage Prediction In Single Point Incremental Forming Using An Extended Gurson Model. *International Journal of Solids and Structures* 151:45–56.

[72] Habibi N, Beier T, Richter H, Könemann M, Münstermann S (2019) The Effects Of Shear Affected Zone On Edge Crack Sensitivity In Dual Phase Steels. In: In: *Proceedings of the 38th International Deep Drawing Research Group Annual Conference*, .

[73] Halim H, Wilkinson DS, Niewczas M (2007) The Portevin-Le Chatelier (PLC) Effect And Shear Band Formation In An AA5754 alloy. *Acta Materialia* 55:4151–4160.

[74] Hambli R (2001) Finite Element Simulation Of Fine Blanking Processes Using A Pressure-Dependent Damage Model. *Journal of Materials Processing Technology* 116:252–264.

[75] Han X, Yang K, Ding Y, Tan S, Chen J (2016) Numerical And Experimental Investigations On Mechanical Trimming Process For Hot Stamped Ultra-High Strength Parts. *Journal of Materials Processing Technology* 234:158–168.

[76] Heibel S, Dettinger T, Nester W, Clausmeyer T, Tekkaya AE (2018) Damage Mechanisms And Mechanical Properties Of High-Strength Multiphase Steels. *Materials* 11/5:761.

[77] Heibel S, Nester W, Clausmeyer T, Tekkaya AE (2017) Failure Assessment In Sheet Metal Forming Using A Phenomenological Damage Model And Fracture Criterion: Experiments, Parameter Identification And Validation. *Procedia Engineering* 207:2066–2071.

[78] Hering O (2020) *Schädigungskontrolliertes Vollvorwärtsfließpressen* Doctoral Thesis. TU Dortmund University.

[79] Hering O, Dunlap A, Tekkaya AE, Aretz A, Schwedt A (2019) Characterization Of Damage In Forward Rod Extruded Parts. *International Journal of Material Forming*. https://doi.org/10.1007/s12289-019-01525-z.

[80] Hering O, Kolpak F, Tekkaya AE (2019) Flow Curves Up To High Strains Considering Load Reversal And Damage. *International Journal of Material Forming* 12:955–972.

[81] Hering O, Tekkaya AE (2020) Damage-Induced Performance Variations Of Cold Forged Parts. *Journal of Materials Processing Technology* 279:116556.

[82] Hoefnagels JPM, Tasan CC, Maresca F, Peters FJ, Kouznetsova VG (2015) Retardation Of Plastic Instability Via Damage-Enabled Microstrain Delocalization. *Journal of Materials Science* 50/21:6882–6897.

[83] Hong SI, Laird C (1991) Faceted Fatigue Fracture And Its Relation To The Crystallographic Slip Systems In Cu-16 at. Pct al Single Crystals. *Metallurgical Transactions A* 22/2:415–425.

[84] Hu P, Shi D, Ying L, Shen G, Liu W (2015) The Finite Element Analysis Of Ductile Damage During Hot Stamping of 22MnB5 Steel. *Materials & Design* 69:141–152.

[85] Huo Y, Lin J, Bai Q, Wang B, Tang X, Ji H (2017) Prediction Of Microstructure And Ductile Damage Of A High-Speed Railway Axle Steel During Cross Wedge Rolling. *Journal of Materials Processing Technology* 239:359–369.

[86] Isik K, Gerstein G, Clausmeyer T, Nürnberger F, Tekkaya AE, Maier HJ (2016) Evaluation Of Void Nucleation And Development During Plastic Deformation Of Dual-Phase Steel DP600. *Steel Research International* 87:1583–1591.

[87] Isik K, Gerstein G, Schneider T, Schulte R, Rosenbusch D, Clausmeyer T, Nürnberger F, Vucetic M, Koch S, Hübner S, Behrens B-A, Tekkaya AE, Merklein M (2016) Investigations Of Ductile Damage During The Process Chains Of Toothed Functional Components Manufactured By Sheet-Bulk Metal Forming. *Production Engineering* 10/1:5–15.

[88] Isik K, Yoshida Y, Chen L, Clausmeyer T, Tekkaya AE (2018) Modelling Of The Blanking Process Of High-Carbon Steel Using Lemaitre Damage Model. *Comptes Rendus Mécanique* 346/8:770–778.

[89] Jablokov V, Goto DM, Koss DA (2001) Damage Accumulation And Failure Of HY-100 Steel. *Metallurgical and Materials Transactions A* 32/12:2985–2994.

[90] Jacques P (2001) On The Role Of Martensitic Transformation On Damage And Cracking Resistance In TRIP-Assisted Multiphase Steels. *Acta Materialia* 49/1:139–152.

[91] Jiang W, Li Y, Su J (2016) Modified GTN Model For A Broad Range Of Stress States And Application To Ductile Fracture. *European Journal of Mechanics - A/Solids* 57:132–148.

[92] Jirásek M (1998) Nonlocal Models For Damage And Fracture: Comparison Of Approaches. *International Journal of Solids and Structures* 35/31–32:4133–4145.

[93] Johnson GR, Cook WH (1985) Fracture Characteristics Of Three Metals Subjected To Various Strains, Strain Rates, Temperatures And Pressures. *Engineering Fracture Mechanics* 21/1:31–48.

[94] Joshi VA (2006) *Titanium Alloys*, CRC PressBoca Raton, FL.

[95] Kacem A, Krichen A, Manach PY, Thuillier S, Yoon JW (2013) Failure Prediction In The Hole-Flanging Process Of Aluminium Alloys. *Engineering Fracture Mechanics* 99:251–265.

[96] Kachanov ML (1958) Time Of The Rupture Process Under Creep Conditions, Izy Akad. *Nank S. S. R. Otd Tech Nauk* 8:26–31.

[97] Kami A, Dariani BM, Sadough Vanini A, Comsa DS, Banabic D (2015) Numerical Determination Of The Forming Limit Curves Of Anisotropic Sheet Metals Using GTN Damage Model. *Journal of Materials Processing Technology* 216:472–483.

[98] El Khaoulani R, Bouchard PO (2012) An Anisotropic Mesh Adaptation Strategy For Damage And Failure In Ductile Materials. *Finite Elements in Analysis and Design* 59:1–10.

[99] Kim S-W, Lee Y-S (2014) Comparative Study On Failure Prediction In Warm Forming Processes Of Mg Alloy Sheet By The FEM and Ductile Fracture Criteria. *Metallurgical and Materials Transactions B* 45/2:445–453.

[100] Koyama M, Springer H, Merzlikin SV, Tsuzaki K, Akiyama E, Raabe D (2014) Hydrogen Embrittlement Associated With Strain Localization In A Precipitation-Hardened Fe-Mn-Al-C Light Weight Austenitic Steel. *International Journal of Hydrogen Energy* 39/9:4634–4646.

[101] Koyama M, Zhang Z, Wang M, Ponge D, Raabe D, Tsuzaki K, Noguchi H, Tasan CC (2017) Bone-Like Crack Resistance In Hierarchical Metastable Nanolaminate Steels. *Science (New York, N.Y.)* 355:1055–1057.

[102] Kumar S, Curtin WA (2007) Crack Interaction With Microstructure. *Materials Today* 10/9:34–44.

[103] Kusche C, Reclik T, Freund M, Al-Samman T, Kerzel U, Korte-Kerzel S (2019) Large-Area, High-Resolution Characterisation And Classification Of Damage Mechanisms In Dual-Phase Steel Using Deep Learning. *PLOS ONE* 14/5: e0216493.

[104] Lai Q, Bouaziz O, Gouné M, Brassart L, Verdier M, Parry G, Perlade A, Bréchet Y, Pardoen T (2015) Damage And Fracture Of Dual-Phase Steels: Influence Of Martensite Volume Fraction. *Materials Science and Engineering: A* 646:322–331.

[105] Lapovok R, Hodgson D (2009) A Damage Accumulation Model For Complex Strain Paths: Prediction Of Ductile Failure In Metals. *Journal of the Mechanics and Physics of Solids* 57/11:1851–1864.

[106] Lapovok R, Mendoza V, Anumalasetty VN, Hodgson PD (2016) Prediction Of Ductile Failure In CP-Titanium as Criterion of SPD Process Design. *Journal of Materials Processing Technology* 229:678–686.

[107] Lassancel D, Fabregue D, Delannay F, Pardoen T (2007) Micromechanics Of Room And High Temperature Fracture In 6xxx Al Alloys. *Progress in Materials Science* 52/1:62–129.

[108] Lee YS, Lee SU, Van Tyne CJ, Joo BD, Moon YH (2011) Internal Void Closure During The Forging Of Large Cast Ingots Using A Simulation Approach. *Journal of Materials Processing Technology* 211/6:1136–1145.

[109] Lemaitre J, Ladevèze P (1984) Damage Effective Stress In Quasi-Unilateral Condition. *IUTAM Congress*, LyngbyDanemark.

[110] Lemaitre J (1985) A Continuous Damage Mechanics Model For Ductile Fracture. *Journal of Engineering Materials and Technology* 107/1:83.

[111] Lemaitre J (1986) Local Approach Of Fracture. *Engineering Fracture Mechanics* 25/5–6:523–537.

[112] Lemaitre J, Desmorat R (2005) *Engineering Damage Mechanics*, Springer-Verlag-Berlin/Heidelberg.

[113] Lemaitre J, Dufailly J (1987) Damage Measurements. *Engineering Fracture Mechanics* 28/5–6:643–661.

[114] León-García Orlando O, Petrov R, Kestens LAI (2010) Void Initiation At TiN Precipitates In IF Steels During Tensile Deformation. *Materials Science and Engineering A* 527/16-17:4202–4209.

[115] Li S, Li Y, Lo Y-C, Neeraj T, Srinivasan R, Ding X, Sun J, Qi L, Gumbsch P, Li J (2015) The Interaction Of Dislocations And Hydrogen-Vacancy Complexes And Its Importance For Deformation-Induced Proto Nano-Voids Formation In α-Fe. *International Journal of Plasticity* 74:175–191.

[116] Li Y, Luo M, Gerlach J, Wierzbicki T (2010) Prediction Of Shear-Induced Fracture In Sheet Metal Forming. *Journal of Materials Processing Technology* 210/14:1858–1869.

[117] Li Z, Pradeep KG, Deng Y, Raabe D, Tasan CC (2016) Metastable High-Entropy Dual-Phase Alloys Overcome The Strength–Ductility Trade-off. *Nature* 534/7606:227–230.

[118] Lian J, Yang H, Vajragupta N, Münstermann S, Bleck W (2014) A Method To Quantitatively Upscale The Damage Initiation Of Dual-Phase Steels Under Various Stress States From Microscale To Macroscale. *Computational Materials Science* 94:245–257.

[119] Lin J, Liu Y, Dean TA (2005) A Review On Damage Mechanisms, Models And Calibration Methods Under Various Deformation Conditions. *International Journal of Damage Mechanics* 14/4:299–319.

[120] Lin YC, Liu Y-X, Liu G, Chen M-S, Huang Y-C (2015) Prediction of Ductile Fracture Behaviors for 42CrMo Steel At Elevated Temperatures. *Journal of Materials Engineering and Performance* 24/1:221–228.

[121] Liu J, Bai Y, Xu C (2013) Evaluation Of Ductile Fracture Models In Finite Element Simulation Of Metal Cutting Processes. *Journal of Manufacturing Science and Engineering* 136/1:011010.

[122] Lode W (1926) Versuche Über Den Einfluß Der Mittleren Hauptspannung Auf Das Fließen der Metalle Eisen, Kupfer und Nickel. *Zeitschrift für Physik* 36/11–12:913–939.

[123] Lou Y, Chen L, Clausmeyer T, Tekkaya AE, Yoon JW (2017) Modeling Of Ductile Fracture From Shear To Balanced Biaxial Tension For Sheet Metals. *International Journal of Solids and Structures* 112:169–184.

[124] Lou Y, Huh H, Lim S, Pack K (2012) New Ductile Fracture Criterion For Prediction Of Fracture Forming Limit Diagrams Of Sheet Metals. *International Journal of Solids and Structures* 49/25:3605–3615.

[125] Lou Y, Yoon JW, Huh H (2014) Modeling Of Shear Ductile Fracture Considering A Changeable Cut-Off Value For Stress Triaxiality. *International Journal of Plasticity* 54:56–80.

[126] Lu XZ, Chan LC (2018) Micro-Voids Quantification For Damage Prediction In Warm Forging Of Biocompatible Alloys Using 3D X-ray CT and RVE Approach. *Journal of Materials Processing Technology* 258:116–127.

[127] Ludwik P (1926) Bestimmung Der Reißfestigkeit Aus Der Gleichmäßigen Dehnung. *Zeitschrift für Metallkunde* 18/9:269–272.

[128] Ludwik P, Scheu R (1923) Über Kerbwirkungen Bei Flußeisen. *Stahl und Eisen* 31/43:999–1001.

[129] Lund JR, Byrne JP (2001) Leonardo Da Vinci's Tensile Strength Tests: Implications For The Discovery Of Engineering Materials. *Civil Engineering and Environmental Systems* 18/3:243–250.

[130] Madou K, Leblond J-B (2012) A Gurson-Type Criterion For Porous Ductile Solids Containing Arbitrary Ellipsoidal Voids—I: Limit-Analysis of Some Representative Cell. *Journal of the Mechanics and Physics of Solids* 60/5:1020–1036.

[131] Maire E, Bouaziz O, Di Michiel M, Verdu C (2008) Initiation And Growth Of Damage In A Dual-Phase Steel Observed By X-ray Microtomography. *Acta Materialia* 56/18:4954–4964.

[132] Maire E, Withers PJ (2013) Quantitative X-Ray Tomography. *International Materials Reviews* 59/1:1–43.

[133] Mandelbrot BB, Passoja DE, Paullay AJ (1984) Fractal Character Of Fracture Surfaces Of Metals. *Nature* 308:721–722.

[134] Marino B, Mudry F, Pineau A (1985) Experimental Study Of Cavity Growth In Ductile Rupture. *Engineering Fracture Mechanics* 22/6:989–996.

[135] Martin ML, Roberstson IMSP (2011) Interpreting Hydrogen-Induced Fracture Surfaces In Terms Of Deformation Processes: A New Approach. *Scripta Materialia* 59/9:3680–3687.

[136] McClintock FA (1968) A Criterion For Ductile Fracture By The Growth Of Holes. *Journal of Applied Mechanics* 35/2:363–371.

[137] McVeigh C, Vernerey F, Liu W, Moran B, Olson G (2007) An Interactive Micro-Void Shear Localization Mechanism In High Strength Steels. *Journal of the Mechanics and Physics of Solids* 55/2:225–244.

[138] Meya R (2020) *Schädigungskontrolliertes Blechbiegen mittels Druckspannungsüberlagerung, Doctoral Thesis*, TU Dortmund University.

[139] Meya R, Kusche C, Löbbe C, Al-Samman T, Korte-Kerzel S, Tekkaya AE (2019) Global And High-Resolution Damage Quantification In Dual-Phase Steel Bending Samples With Varying Stress States. *Metals* 9/3:319.

[140] Meya R, Löbbe C, Tekkaya AE (2019) Stress State Control By A Novel Bending Process And Its Effect On Damage And Product Performance. *Journal of Manufacturing Science and Engineering* 141/10.

[141] Meya R, Löbbe C, Tekkaya AE (2018) Stress State Control By A Novel Bending Process And Its Effect On Damage Evolution. In: In: *Proceedings of the 2018 Manufacturing Science and Engineering Conference MSEC*, .

[142] Meya R, Löbbe C, Tekkaya AE (2019) Stress State Analysis Of Radial Stress Superposed Bending. *International Journal of Precision Engineering and Manufacturing* 20/1:53–66.

[143] Mirahmadi SJ, Hamedi M, Ajami S (2014) Investigating The Effects Of Cross Wedge Rolling Tool Parameters On Formability Of Nimonic® 80a And Nimonic® 115 Superalloys. *The International Journal of Advanced Manufacturing Technology* 74/5:995–1004.

[144] Mirnia MJ, Shamsari M (2017) Numerical Prediction Of Failure In Single Point Incremental Forming Using A Phenomenological Ductile Fracture Criterion. *Journal of Materials Processing Technology* 244:17–43.

[145] Mohr D, Marcadet SJ (2015) Micromechanically-Motivated Phenomenological Hosford–Coulomb Model For Predicting Ductile Fracture Initiation At Low Stress Triaxialities. *International Journal of Solids and Structures* 67–68:40–55.

[146] Mohrbacher H (2008) Delayed Cracking In Ultra-High Strength Automotive Steels: Damage Mechanisms And Remedies By Microstructural Engineering. In: In: *Proceedings of the Materials Science and Technology Conference and Exhibition*, . MS and T'08.

[147] Mohrbacher H (2013) Reverse Metallurgical Engineering Towards Sustainable Manufacturing Of Vehicles Using NB And MO Alloyed High Performance Steels. *Advances in Manufacturing* 1/1:28–41.

[148] Morales-Rivas L, Yen HW, Huang BM, Kuntz M, Caballero FG, Yang JR, Garcia-Mateo C (2015) Tensile Response Of Two Nanoscale Bainite Composite-Like Structures. *JOM* 67/10:2223–2235.

[149] Morgeneyer TF, Taillandier-Thomas T, Helfen L, Baumbach T, Sinclair I, Roux S, Hild F (2014) In Situ 3-D Observation Of Early Strain Localization During Failure Of Thin Al Alloy (2198) Sheet. *Acta Materialia* 69:78–91.

[150] Nahshon K, Hutchinson JW (2008) Modification of the Gurson Model For Shear Failure. *European Journal of Mechanics - A/Solids* 27/1:1–17.

[151] Needleman A., Toughness, Roughness And The Possibility Of Microstructure Design For Improved Crack Growth Resistance, *Plenary Talk, The 13th International Conference on Numerical Methods in Industrial Forming Processes, Portsmouth, USA*, 2019.

[152] Noell PJ, Carroll JD, Boyce BL (2018) The Mechanisms Of Ductile Rupture. *Acta Materialia* 161:83–98.

[153] Novella MF, Ghiotti A, Bruschi S, Bariani PF (2015) Ductile Damage Modeling At Elevated Temperature Applied To The Cross Wedge Rolling Of AA6082-T6 Bars. *Journal of Materials Processing Technology* 222:259–267.

[154] Odette GR, Alinger MJ, Wirth BD (2008) Recent Developments In Irradiation-Resistant Steels. *Annual Review of Materials Research* 38:471–503.

[155] Oliver WC, Pharr GM (2004) Measurement Of Hardness And Elastic Modulus By Instrumented Indentation: Advances In Understanding And Refinements To Methodology. *Journal of Materials Research* 19/1:3–20.

[156] Oyane M, Sato T, Okimoto K, Shima S (1980) Criteria For Ductile Fracture And Their Applications. *Journal of Mechanical Working Technology* 4/1:65–81.

[157] Pathak N, Butcher C, Worswick M, Bellhouse E, Gao J (2017) Damage Evolution In Complex-Phase And Dual-Phase Steels During Edge Stretching. *Materials* 10/4:346.

[158] Peerlings RHJ, De Borst R, Brekelmans WAM, De Vree JHP (1996) Gradient Enhanced Damage For Quasi-Brittle Materials. *International Journal for Numerical Methods in Engineering* 39/19:3391–3403.

[159] Peerlings RHJ, Geers MGD, de Borst R, Brekelmans WAM (2001) A Critical Comparison Of Nonlocal And Gradient-Enhanced Softening Continua. *International Journal of Solids and Structures* 38/44–45:7723–7746.

[160] Pineau A, Benzerga AA, Pardoen T (2016) Failure Of Metals I: Brittle And Ductile Fracture. *Acta Materialia* 107:424–483.

[161] Pirondi A, Bonora N (2003) Modeling Ductile Damage Under Fully Reversed Cycling. *Computational Materials Science* 26:129–141.

[162] Remmers WE (1930) Causes Of Cuppy Wire. *Transactions of the Metallurgical Society of AIME* 89:107–120.

[163] Rice JR, Tracey DM (1969) On The Ductile Enlargement Of Voids In Triaxial Stress Fields. *Journal of the Mechanics and Physics of Solids* 17/3:201–217.

[164] Roth CC, Mohr D (2014) Effect Of Strain Rate On Ductile Fracture Initiation In Advanced High Strength Steel Sheets: Experiments And Modeling. *International Journal of Plasticity* 56:19–44.

[165] Roth CC, Morgeneyer TF, Cheng Y, Helfen L, Mohr D (2018) Ductile Damage Mechanism Under Shear-Dominated Loading: In-Situ Tomography Experiments

On Dual Phase Steel And Localization Analysis. *International Journal of Plasticity* 109:169–192.
[166] Rousselier G (1987) Ductile Fracture Models And Their Potential In Local Approach Of Fracture. *Nuclear Engineering and Design* 105/1:97–111.
[167] Roux E, Bouchard P-O (2013) Kriging Metamodel Global Optimization Of Clinching Joining Processes Accounting For Ductile Damage. *Journal of Materials Processing Technology* 213/7:1038–1047.
[168] Roux E, Bouchard P-O (2015) On The Interest Of Using Full Field Measurements In Ductile Damage Model Calibration. *International Journal of Solids and Structures* 72:50–62.
[169] Roux E, Shakoor M, Bernacki M, Bouchard P-O (2014) A New Finite Element Approach For Modelling Ductile Damage Void Nucleation And Growth—Analysis Of Loading Path Effect On Damage Mechanisms. *Modelling and Simulation in Materials Science and Engineering* 22/7:075001.
[170] Rüf G, Sommitsch C, Buchmayr B (2007) On The Interaction Of Ductile Damage And Materials Softening Of A Ni-Base Alloy During Hot Deformation. *International Journal of Materials Research* 98/11:1146–1155.
[171] Saanouni K, Mariage JF, Cherouat A, Lestriez P (2004) Numerical Prediction Of Discontinuous Central Bursting In Axisymmetric Forward Extrusion By Continuum Damage Mechanics. *Computers and Structures* 82/27:2309–2332.
[172] Saboori M, Gholipour J, Champliaud H, Wanjara P, Gakwaya A, Savoie J (2016) Prediction Of Burst Pressure In Multistage Tube Hydroforming Of Aerospace Alloys. *Journal of Engineering for Gas Turbines and Power* 138/8.
[173] Saby M, Bernacki M, Roux E, Bouchard P-O (2013) Three-Dimensional Analysis Of Real Void Closure At The Meso-Scale During Hot Metal Forming Processes. *Computational Materials Science* 77:194–201.
[174] Saby M, Bouchard P-O, Bernacki M (2015) Void Closure Criteria For Hot Metal Forming: A Review. *Journal of Manufacturing Processes* 19:239–250.
[175] Sahu JK, Krupp U, Ghosh RN, Christ H-J (2009) Effect of 475°C Embrittlement On The Mechanical Properties Of Duplex Stainless Steel. *Materials Science and Engineering: A* 508/1–2:1–14.
[176] Sari Sarraf I, Green DE, Vasilescu DM, Song Y (2018) Numerical Analysis Of Damage Evolution And Formability Of DP600 Sheet With An Extended Rousselier Damage Model. *International Journal of Solids and Structures* 134:70–88.
[177] Schowtjak A, Kusche CF, Meya R, Al-Samman T, Korte-Kerzel S, Tekkaya AE, Clausmeyer T (2019) Prediction Of Void Evolution In Sheet Bending Based On Statistically Representative Microstructural Data For The Gurson-Tvergaard-Needleman Model. In: *Proceedings of NUMIFORM 2019, Portsmouth, USA*: 311–314.
[178] Schowtjak A, Wang S, Hering O, Clausmeyer T, Lohmar J, Schulte R, Ostwald R, Hirt G, Tekkaya AE (2020) Prediction And Analysis Of Damage Evolution During Caliber Rolling And Subsequent Cold Forward Extrusion. *Production Engineering* 14/1:33–41.
[179] Schwab W, Lange K (1985) Effect Of Process Parameters In Metalforming On Fatigue Behaviour. *CIRP Annals* 34/1:215–219.
[180] Shabrov MN, Briant CL, Needleman A, Kim S, Sylven E, Sherman DH, Chuzhoy L (2004) Void Nucleation By Inclusion Cracking. *Metallurgical and Materials Transactions A* 35/6:1745–1755.
[181] Shakoor M, Bernacki M, Bouchard P-O (2015) A New Body-Fitted Immersed Volume Method For The Modeling Of Ductile Fracture At The Microscale: Analysis Of Void Clusters And Stress State Effects On Coalescence. *Engineering Fracture Mechanics* 147:398–417.
[182] Shakoor M, Trejo Navas VM, Pino Munõz D, Bernacki M, Bouchard P-O (2019) Computational Methods For Ductile Fracture Modeling At The Microscale. *Archives of Computational Methods in Engineering* 26/4:1153–1192.
[183] Sizova I, Bambach M (2018) Hot Workability And Microstructure Evolution Of Pre-Forms For Forgings Produced By Additive Manufacturing. *Journal of Materials Processing Technology* 256:154–159.
[184] Soyarslan C, Malekipour Gharbi M, Tekkaya AE (2012) A Combined Experimental–Numerical Investigation Of Ductile Fracture In Bending Of A Class Of Ferritic–Martensitic Steel. *International Journal of Solids and Structures* 49/13:1608–1626.
[185] Soyarslan C, Tekkaya AE (2010) Finite Deformation Plasticity Coupled With Isotropic Damage: Formulation In Principal Axes And Applications. *Finite Elements in Analysis and Design* 46/8:668–683.
[186] Sprave L, Schowtjak A, Meya R, Clausmeyer T, Tekkaya AE, Menzel A (2020) On Mesh Dependencies In Finite-Element-Based Damage Prediction: Application To Sheet Metal Bending. *Production Engineering* 14/1:123–134.
[187] Suárez F, Sket F, Gálvez J, Cendón D, Atienza J, Molina-Aldareguia J (2019) The Evolution Of Internal Damage Identified By Means Of X-Ray Computed Tomography In Two Steels And The Ensuing Relation With Gurson's Numerical Modelling. *Metals* 9/3:292.
[188] Tang BT, Bruschi S, Ghiotti A, Bariani PF (2016) An Improved Damage Evolution Model To Predict Fracture Of Steel Sheet At Elevated Temperature. *Journal of Materials Processing Technology* 228:76–87.
[189] Tasan CC, Diehl M, Yan D, Zambaldi C, Shanthraj P, Roters F, Raabe D (2014) Integrated Experimental-Simulation Analysis Of Stress And Strain Partitioning In Multiphase Alloys. *Acta Materialia* 81:386–400.
[190] Tasan CC, Hoefnagels JPM, ten Horn CHLJ, Geers MGD (2009) Experimental Analysis Of Strain Path Dependent Ductile Damage Mechanics And Forming limits. *Mechanics of Materials* 41/11:1264–1276.
[191] Tasan CC, Diehl M, Yan D, Bechtold M, Roters F, Schemmann L, Zheng C, Peranio N, Ponge D, Koyama M, Tsuzaki K, Raabe D (2015) An Overview Of Dual-Phase Steels: Advances In Microstructure-Oriented Processing And Micromechanically Guided Design. *Annual Review of Materials Research* 45/1:391–431.
[192] Tasan CC, Hoefnagels JPM, Diehl M (2014) Strain Localization And Damage In Dual Phase Steels Investigated By Coupled In-Situ Deformation Experiments And Crystal Plasticity Simulations. *International Journal of Plasticity* 63:198–210.
[193] Tasan CC, Hoefnagels JPM, Geers MGD (2009) A Critical Assessment Of Indentation-Based Ductile Damage Quantification. *Acta Materialia* 57/17:4957–4966.
[194] Tasan CC, Hoefnagels JPM, Geers MGD (2012) Identification Of The Continuum Damage Parameter: An Experimental Challenge In Modeling Damage Evolution. *Acta Materialia* 60/8:3581–3589.
[195] Tasan CC, Hoefnagels JPM, Geers MGD (2010) Indentation-Based Damage Quantification Revisited. *Scripta Materialia* 63/3:316–319.
[196] Tehranchi A, Yin B, Curtin WA (2017) Softening And Hardening Of Yield Stress By Hydrogen–Solute Interactions. *Philosophical Magazine* 97/6:400–418.
[197] Teixeira P, Santos AD, Andrade Pires FM, César de Sá JMA (2006) Finite Element Prediction Of Ductile Fracture In Sheet Metal Forming Processes. *Journal of Materials Processing Technology* 177/1–3:278–281.
[198] Tekkaya AE, Ben Khalifa N, Hering O, Meya R, Myslicki S, Walther F (2017) Forming-Induced Damage And Its Effects On Product Properties. *CIRP Annals - Manufacturing Technology* 66/1:281–284.
[199] Tekkaya AE, Allwood JM, Bariani PF, Bruschi S, Cao J, Gramlich S, Groche P, Hirt G, Ishikawa T, Löbbe C, Lueg-Althoff J, Merklein M, Misiolek WZ, Pietrzyk M, Shivpuri R, Yanagimoto J (2015) Metal forming Beyond Shaping: Predicting And Setting Product Properties. *CIRP Annals - Manufacturing Technology* 64/2:629–653.
[200] Tipper CF (1949) The Fracture Of Metals. *Metallurgia* 39/231:133–137.
[201] Toda H, Kamiko T, Tanabe Y, Kobayashi M, Leclere DJ, Uesugi K, Takeuchi A, Hirayama K (2016) Diffraction-Amalgamated Grain Boundary Tracking For Mapping 3D Crystallographic Orientation And Strain Fields During Plastic Deformation. *Acta Materialia* 107:310–324.
[202] Toda H, Takijiri A, Azuma M, Yabu S, Hayashi K, Seo D, Kobayashi M, Hirayama K, Takeuchi A, Uesugi K (2017) Damage Micromechanisms In Dual-Phase Steel Investigated With Combined Phase- And Absorption-Contrast Tomography. *Acta Materialia* 126:401–412.
[203] Tomota YO, Tamura I (1982) Mechanical Behavior Of Steels Consisting Of Two Ductile Phases. *Transactions of the Iron and Steel Institute of Japan* : 665–677. V 22/N 9.
[204] Toribio J, Kharin V (2004) Role Of Crack Tip Mechanics In Stress Corrosion Cracking of High-Strength Steels. *International Journal of Fracture* 126/3:57–63.
[205] Traphöner H, Clausmeyer T, Tekkaya AE (2017) Material Characterization For Plane And Curved Sheets Using The In-Plane Torsion Test – An Overview. *Procedia Engineering* 207:1934–1939.
[206] Traphöner H, Heibel S, Clausmeyer T, Tekkaya AE (2018) Influence Of Manufacturing Processes On Material Characterization With The Grooved In-Plane Torsion Test. *International Journal of Mechanical Sciences* 146–147:544–555.
[207] Trejo Navas V (2018) A Numerical Study Of The Micromechanisms Of Ductile Damage In Heterogeneous Microstructure, PhD. *Mines ParisTech* .
[208] Tvergaard V, Needleman A (1984) Analysis Of The Cup-Cone Fracture In A Round Tensile Bar. *Acta Metallurgica* 32/1:157–169.
[209] Valoppi B, Bruschi S, Ghiotti A, Shivpuri R (2017) Johnson-Cook Based Criterion Incorporating Stress Triaxiality And Deviatoric Effect For Predicting Elevated Temperature Ductility Of Titanium Alloy Sheets. *International Journal of Mechanical Sciences* 123:94–105.
[210] Wang C, Geijselaers HJM, Omerspahic E, Recina V, van den Boogaard AH (2016) Influence Of Ring Growth Rate On Damage Development In Hot Ring Rolling. *Journal of Materials Processing Technology* 227:268–280.
[211] Wang M-M, Tasan CC, Koyama M, Ponge D, Raabe D (2015) Enhancing Hydrogen Embrittlement Resistance Of Lath Martensite By Introducing Nano-Films Of Interlath Austenite. *Metallurgical and Materials Transactions* 46/9:3797–3802.
[212] Wang MM, Hell JC, Tasan CC (2017) Martensite Size Effects On Damage In Quenching And Partitioning Steels. *Scripta Materialia* 138:1–5.
[213] Wang S, Dunlap A, Möhring K, Lohmar J, Schwedt A, Aretz A, Walther F, Hirt G (2020) Torsion Plastometer Trails To Investigate The Effect Of The Non-Proportional Load Path In Caliber Rolling On Damage And Performance In Metal Parts. *Production Engineering* 14/1:17–32.
[214] Webster GA, Ezeilo AN (2001) Residual Stress Distributions And Their Influence On Fatigue Lifetimes. *International Journal of Fatigue* 23/1:375–383.
[215] Weck A, Wilkinson DS, Maire E, Toda H (2008) Visualization by X-ray Tomography Of Void Growth And Coalescence Leading To Fracture In Model Materials. *Acta Materialia* 56/12:2919–2928.
[216] Wierzbicki T, Bao Y, Lee Y-W, Bai Y (2005) Calibration And Evaluation Of Seven Fracture Models. *International Journal of Mechanical Sciences* 47/4–5:719–743.
[217] Xue L (2008) Constitutive Modeling Of Void Shearing Effect In Ductile Fracture Of Porous Materials. *Engineering Fracture Mechanics* 75/11:3343–3366.
[218] Yan D, Tasan CC, Raabe D (2015) High Resolution In Situ Mapping Of Microstrain And Microstructure Evolution Reveals Damage Resistance Criteria In Dual Phase Steels. *Acta Materialia* 96:399–409.
[219] Yoon JI, Jung J, Lee HH, Kim G-S, Kim HS (2016) Factors Governing Hole Expansion Ratio Of Steel Sheets With Smooth Sheared Edge. *Metals and Materials International* 22/6:1009–1014.
[220] Zeng D, Liu SD, Makam V, Shetty S, Zhang L, Zweng F (2002) Specifying Steel Properties And Incorporating Forming Effects In Full Vehicle Impact Simulation. *SAE Transactions* 111:398–404.
[221] Zhan M, Guo J, Fu MW, Gao PF, Long H, Ma F (2018) Formability Limits And Process Window Based On Fracture Analysis Of 5a02-O Aluminium Alloy In Splitting Spinning. *Journal of Materials Processing Technology* 257:15–32.
[222] Zheng J, Lou Y, Zhu X, Sang S, Yoon JW (2019) LS-DYNA Material Model 263 And Its Application To Earing Predictions In Cup-Drawing. In: In: *Proceedings of LSTC China Conference*, .
[223] Zinkle SJ, Busby JT (2009) Structural Materials For Fission And Fusion Energy. *Materials Today* 12/11:12–19.